# JCTC Journal of Chemical Theory and Computation

# Comprehensive Energy Analysis for Various Types of $\pi$-Interaction

N. Jiten Singh, Seung Kyu Min, Dong Young Kim, and Kwang S. Kim*

*Center for Superfunctional Materials, Department of Chemistry, Pohang University of Science and Technology, Pohang 790-784, Korea*

**Abstract:** We have investigated various types of $\pi$-interactions, where one of the interacting $\pi$-systems is represented by an aromatic benzene molecule. The system includes Rg-$\pi$, CH-$\pi$, $\pi$-$\pi$(D), $\pi$-$\pi$(T), H-$\pi$(T), $\pi^+$-$\pi$(D), $\pi^+$-$\pi$(T), H$^+$-$\pi$(T), $\pi^{+2}$-$\pi$(D), M$^+$-$\pi$, and M$^{+2}$-$\pi$ complexes, where Rg denotes a rare gas or noble atom, M denotes a metal, and D/T indicates displaced-stacked/T-shaped structure. The microsolvation effect is also considered. We note that the interaction between a cationic $\pi$ system and a neutral $\pi$ system ($\pi_{cation}$-$\pi$ interaction) is so far ambiguously considered as either $\pi$-$\pi$ or cation-$\pi$ interaction. In terms of total binding energy, the $\pi_{cation}$-$\pi$ interaction is weaker than the cation$-\pi$ interaction, but much stronger than the $\pi$-$\pi$ interaction. When the hydrophilic (N$-$H)$^+$ or (C$-$H)$^+$ group in a singly charged $\pi^+$ system (as in protonated histidine, arginine, pyridine, or dimethyl imidazolium) interacts with a $\pi$-system, the complex favors a T-shaped form [$\pi^+$-$\pi$(T) complex]. However, in the presence of polar solvating molecules or counteranions, these species interact with the (N$-$H)$^+$/(C$-$H)$^+$ group, while the $\pi^+$ system interacts with the neutral aromatic ring. Then, the displaced-stacked form [$\pi^+$-$\pi$(D) complex] is favored or otherwise nearly isoenergetic to the $\pi^+$-$\pi$(T) form. The $\pi^+$-$\pi$ systems are stabilized mainly by both dispersion and electrostatic energies. Ternary diagrams using either attractive energy components or both attractive and repulsive energy components show that the $\pi^+$-$\pi$(D) complexes have more contribution from dispersion energy but less contribution from induction energy than the $\pi^+$-$\pi$(T) complexes, while both complexes have similar percentage contributions from electrostatic and exchange energy components. In particular, the $\pi^+$-$\pi$(D) complexes are found to be distinctly different from the $\pi$-$\pi$ complexes and the non-$\pi$ organic or metallic cation-$\pi$ complexes.

## 1. Introduction

Nonbonding intermolecular interactions involving aromatic rings[1−5] are pivotal to the stabilization of proteins, enzyme$-$drug complexes, DNA$-$protein complexes, organic supramolecules, and nanomaterials.[1−11] In the last two decades, extensive studies have been done to understand the nature of $\pi$-complexes including the Rg-$\pi$ interaction,[12,13] H-$\pi$/CH-$\pi$ interaction,[6,14,17−22] $\pi$-$\pi$ interaction,[7,23−43] cation-$\pi$ interaction,[44−52] and anion-$\pi$ interaction.[53−57] Extensive investigations have been made on the energetic and geometrical significance of $\pi$-interactions in stabilizing $\pi$ systems.[58−85] Theoretical interpretations based on high level ab initio calculations have been instrumental in understanding the nature of $\pi$-interactions. The strength of the $\pi$-interactions is determined by the combined effect of attractive forces (electrostatic, dispersive, and inductive) and repulsive forces (exchange repulsion). Each of these components shows distinguished differences in physical origin, magnitude, and directionality. The dominant attractive energy component in the $\pi$-$\pi$ interaction is the dispersion energy,[23,37,43,68] while that in the cation-$\pi$ interaction is the electrostatic and induction energies.[44−52]

Interactions between the cationic $\pi$-systems ($\pi_{cation}$) and neutral $\pi$ systems are present in many biological and

* Correponding Author e-mail: kim@postech.ac.kr.

macromolecular systems and organic and metallo-organic systems. For example, the interactions play a pivotal role in various ways like (i) forming protein−drug complexes,[86−92] (ii) stabilizing proteins, particularly protein surfaces,[93−95] (iii) stabilizing protein−protein complexes,[96,97] (iv) assisting catalytic activities at the catalytic site of proteins,[96,97] (v) stabilizing protein−DNA complexes,[98,99] (vi) molecule-recognizing artificial receptors for neutral or π-cationic guests,[100,101] (vii) interlocking macromolecules in molecular machines,[102,103] (viii) self-assembling supramolecular structures and packing crystal structures,[104,105] and (ix) controlling conformations in regio- and stereoselective organic synthesis.[106,107]

In experiments, the concept of host−guest interaction between a neutral aromatic ring (benzene and naphthalene derivatives or tetrathiafulvalene) and the tetracationic cyclophane[100,101] has been explored as a fundamental component in constructing diverse catenanes and rotaxanes.[102,103] Upon interacting with a π-system, the quinolinium cation is bound to it more strongly than quinoline.[108] Nitrogen-containing aromatic cations are widely used for room temperature ionic liquids[109,110] as well as anion recognition.[111,112] The π-aromatic ring of triclosan, a general purpose biocide, interacts strongly with a positively charged nicotinamide ring of nicotinamide adenine dinucleotide(NAD$^+$) located in the active site of enoyl-acyl carrier protein reductase (ENR).[86] In protein structures, the interactions of neutral aromatic amino acids (Phe, Tyr, Trp) with a positively charged π-cloud of arginine are more commonly observed than those with cationic lysine, and their stacked geometries are preferred over the T-shaped structures,[114] whereas in the gas phase the T-shaped structures are more stable. In many of the proteins and protein−ligand complexes, both T-shaped and displaced-stacked structures are equally observed for the interactions of a positively charged histidine residue with the Phe, Tyr, Trp, or Ade residues.[115] It is not yet clearly understood why stacked structures are much more common. The interaction between benzene and pyridinium/imidazolium was suggested as the cation-π interaction[116] where the large dispersion energy term was addressed. However, ambiguity remains whether the interaction between a cationic π-system and a neutral π system would be treated as either conventional cation-π interaction or π-π interaction. Here, we report that it needs to be described as a special type to be denoted by the $\pi_{cation}$-$\pi$ interaction. In particular, the interaction in $\pi^+$-$\pi$(D) complexes (to be denoted simply as the $\pi^+$-$\pi$(D) interaction) cannot be described simply as the cation-π interaction or the π-π interaction.[117,118] This finding is based on the comprehensive analysis of interaction energy components for the Rg-$\pi$, CH-$\pi$, $\pi$-$\pi$(D), $\pi$-$\pi$(T), H-$\pi$(T), $\pi^+$-$\pi$(D), $\pi^+$-$\pi$(T), H$^+$-$\pi$(T), $\pi^{+2}$-$\pi$(D), M$^+$-$\pi$, and M$^{+2}$-$\pi$ complexes.

## 2. Computational Methods

The geometries of complexes were optimized at the basis-set-superposition−error (BSSE) corrected MP2 level of theory using the aug-cc-pVDZ basis set (to be abbreviated as aVDZ). The lowest energy structures were found from the investigation of the energies of various structures with

respect to distances and angles (Supporting Information). These were further calculated using the MP2/aug-cc-pVTZ (to be abbreviated as aVTZ). The complete basis set (CBS) limit values for the MP2 binding energies were evaluated based on the extrapolation method exploiting that the basis set error in the electron correlation energy is proportional to $N^{-3}$ for the aug-cc-pV$N$Z (or aV$N$Z) basis set.[119] Though most extrapolation methods would not be free from inherent over/under−estimation problems, the extrapolation method based on the theoretical understanding is found to be quite reliable.[120] The single point energies using the coupled cluster theory with single, double, and perturbative triple excitations (CCSD(T)) with the aVDZ basis set were also obtained on the BSSE-corrected MP2/aVDZ geometries. Given that the difference in binding energy between MP2/aV$N$Z and CCSD(T)/aV$N$Z does not change significantly with increasing basis set size, the CCSD(T)/CBS binding energies were evaluated from the MP2/CBS ones using the difference between CCSD(T)/aVDZ and MP2/aVDZ binding energies.[120] Ab initio calculations were done using the Gaussian suite of programs[121] (for MP2 calculations) and Molpro package[122] (for CCSD(T) calculations). Symmetry adapted perturbation theory (SAPT) calculations[123,124] at the MP2/6−31+G* or MP2/aVDZ$^†$ (where $^†$ means the diffuse basis function of H was removed from the full aug-cc-pVDZ basis set) level were carried out to evaluate the energy components.

The decomposition for the total interaction energy ($E_{tot}$) is made as follows:[124,125]

$$E_{tot} = E_{es} + E_{exch} + E_{ind} + E_{disp} + \delta_{int,resp}^{HF}$$
$$= E_{es} + E_{exch}* + E_{ind*} + E_{disp*} + \delta_{int,resp}^{HF} \quad (1)$$

where

$$E_{es} = E_{es}^{(10)} + E_{es,resp}^{(12)} \quad (2)$$

$$E_{ind} = E_{ind}^{(20)} \quad (3)$$

$$E_{disp} = E_{disp}^{(20)} \quad (4)$$

$$E_{exch} = E_{exch}^{(10)} + E_{exch}^{(11)} + E_{exch}^{(12)} + E_{exch,ind,resp}^{(20)} + E_{exch,disp}^{(20)} \quad (5)$$

Here, the first number 1 or 2 in parentheses in superscript indicates the first or second order perturbation term; the second number 0/1/2 in parentheses in superscript indicates the zeroth/first/second order correction; Notation "resp" in subscript indicates that a given component has been computed including the coupled Hartree−Fock response for the perturbed system. As in our earlier work[16,43,57] and others,[125] the modified decomposition for the interaction energy ($E_{tot}$) (in which the superscript "*" indicates the effective energy component) is made as follows:

$$E_{ind*} = E_{ind}^{(20)} + E_{exch,ind,resp}^{(20)} + \delta_{int,resp}^{HF} \quad (6)$$

$$E_{disp*} = E_{disp}^{(20)} + E_{exch,disp}^{(20)} \quad (7)$$

$$E_{exch*} = E_{exch}^{(10)} + E_{exch}^{(11)} + E_{exch}^{(12)} \quad (8)$$

Although $E_{ind}$, $E_{disp}$ and $E_{exch}$ are well defined, we need to use $E_{ind*}$, $E_{disp*}$, and $E_{exch*}$ to properly classify different types of π-interactions, i.e., for the purpose of better clustering each characteristic type. To this end, the $\delta_{int,resp}^{HF}$ is added

Comprehensive Energy Analysis for $\pi$-Interaction

*J. Chem. Theory Comput., Vol. 5, No. 3, 2009* **517**

to $E_{\text{ind*}}$, while it is not directly related to the induction but still more correlated to the induction than other terms.

According to our previous investigations for $\pi$-$\pi$ interactions, we note that the base set dependency of $E_{\text{es}}$, $E_{\text{ind*}}$, and $E_{\text{exch*}}$ is small, while that of $E_{\text{disp*}}$ is substantial.[16] Thus, the realistic $E_{\text{disp**}}$ for $\pi$-$\pi$ interactions is obtained by adding the difference between the CCSD(T)/CBS and SAPT(MP2/6-31+G*) interaction energies to $E_{\text{disp*}}$.[43] However, we find that $E_{\text{ind*}}$ needs to be corrected in the case of strongly cationic types of $\pi$-interactions. Hence, we use the following general formula which is applicable to all of the $\pi$-complexes to calculate the respective realistic energy components with respect to the $E_{\text{tot}}$(CCSD(T)/CBS).

$$E_{\text{disp**}} = E_{\text{disp*}}(\text{SAPT(MP2)/basis}) + \kappa_{\text{disp}}(E_{\text{tot}}(\text{CCSD(T)/CBS}) - E_{\text{tot}}(\text{SAPT(MP2)/basis})) \quad (9)$$

$$E_{\text{ind**}} = E_{\text{ind*}}(\text{SAPT(MP2)/basis}) + \kappa_{\text{ind}}(E_{\text{tot}}(\text{CCSD(T)/CBS}) - E_{\text{tot}}(\text{SAPT(MP2)/basis})) \quad (10)$$

On the basis of energy values from SAPT(MP2)/small basis and SAPT(MP2)/large basis, we calculate the ratios of the energy component changes to the total energy changes (denoted by $\kappa_{\text{disp}}$ and $\kappa_{\text{ind}}$ for the dispersion and induction terms). There are insignificant changes in the electrostatic and exchange energy components in all $\pi$-complexes (Table S1 of the Supporting Information). In general, in the neutral $\pi$ complexes and the charged $\pi^+$-$\pi$ complexes, almost solely the dispersion energy is underestimated, while in highly cationic $\pi$ complexes (i.e., multiply charged cations such as $Mg^{2+}$ and $Ca^{2+}$ and highly ionizable cations such as $Li^+$ and $Na^+$ at a very short distance from the benzene molecule) the induction energies are underestimated. Hence, $\kappa_{\text{disp}}/\kappa_{\text{ind}}$ ($\kappa_{\text{disp}} + \kappa_{\text{ind}} = 1$) ranges from 0 to 1 depending on the nature of $\pi$-complexes. In Rg-$\pi$, CH-$\pi$, $\pi$-$\pi$, $\pi$-$\pi$, and $\pi^+$-$\pi$ complexes, $\kappa_{\text{disp}}$ is 1, while $\kappa_{\text{ind}}$ is 0. For the Rg-$\pi$, CH-$\pi$, $\pi$-$\pi$ and $\pi^+$-$\pi$, $\pi^{+2}$-$\pi$ and H-$\pi$ complexes, only the dispersion energy terms show significant changes; thus, $\kappa_{\text{disp}} = 1$ and $\kappa_{\text{ind}} = 0$. For the $NH_4$−benzene complex (H$^+$-$\pi$ complex), $\kappa_{\text{ind}}$ is 0.5 and $\kappa_{\text{disp}}$ is 0.5. On the other hand, for the $Me_4N^+$ complex, which has three methyl groups interacting with the $\pi$-system, $\kappa_{\text{disp}}$ is 1 and $\kappa_{\text{ind}}$ is 0, as in the CH-$\pi$ system. The $\kappa$ values in the M$^+$-$\pi$ and M$^{+2}$-$\pi$ complexes depend on the size of the cation. For the Cs$^+$-$\pi$ complex, $\kappa_{\text{disp}} = 1$ and $\kappa_{\text{ind}} = 0$; for the K$^+$-$\pi$ complex, $\kappa_{\text{disp}} = 0.6$ and $\kappa_{\text{ind}} = 0.4$; for the Na$^+$-$\pi$ complex, $\kappa_{\text{disp}} = 0.4$ and $\kappa_{\text{ind}} = 0.6$; for the Li$^+$-$\pi$ complex, $\kappa_{\text{disp}} = 0.1$ and $\kappa_{\text{ind}} = 0.9$. For the Ca$^{2+}$-benzene complex, $\kappa_{\text{disp}} = 0.2$ and $\kappa_{\text{ind}} = 0.8$; for the Mg$^{2+}$-benzene complex, $\kappa_{\text{disp}} = 0$ and $\kappa_{\text{ind}} = 1$. The details of the proper $\kappa$ values are in the Supporting Information. All of these estimations are used to obtain more realistic values toward the CCSD(T)/CBS limit. However, it should be noted that the corrections are not substantial, and so the raw data without such corrections do not significantly change our results.

We also investigated the ternary diagram analysis for energy component percentages (fractions in %) with respect to $E_{\text{attr}}$ ($= E_{\text{es}} + E_{\text{ind**}} + E_{\text{disp**}}$), which are defined as $f_{\text{es}} =$ $E_{\text{es}}/E_{\text{attr}}$, $f_{\text{ind}} = E_{\text{ind**}}/E_{\text{attr}}$, $f_{\text{disp}} = E_{\text{disp**}}/E_{\text{attr}}$, and $f_{\text{exch}} = -E_{\text{exch*}}/E_{\text{attr}}$. In addition, another set of energy component percentages (fractions in %) is also investigated in consideration of all the attractive and repulsive energy components; $f'_{\text{es,ind}} = (E_{\text{es}} + E_{\text{ind**}})/(E_{\text{attr}} - E_{\text{exch**}})$, $f'_{\text{disp}} = E_{\text{disp**}}/(E_{\text{attr}} - E_{\text{exch*}})$, and $f'_{\text{exch}} = -E_{\text{exch*}}/(E_{\text{attr}} - E_{\text{exch*}})$. For the proper classification of the $\pi$-interactions, the clustering technique is very important, and so a few well-chosen characteristic parameters (which could be represented by a linear or nonlinear combination of well-known physical quantities) should be sought out. Indeed, we note that energy component percentages are also useful parameters.

## 3. Results and Discussion

**A. Model Systems of Various Types of $\pi$-Interactions.** We have chosen various model systems for the Rg-$\pi$, CH-$\pi$, $\pi$-$\pi$(D), $\pi$-$\pi$(T), H-$\pi$(T), $\pi^+$-$\pi$(D), $\pi^+$-$\pi$(T), H$^+$-$\pi$(T), $\pi^{+2}$-$\pi$(D), M$^+$-$\pi$, and M$^{+2}$-$\pi$ complexes (Figure 1), where diverse molecular species interact with a benzene molecule as simplified examples of these very complex systems. Since the electron-rich benzene is not interacting with anions, the electron-deficient $\pi$ systems involving in the anion-$\pi$ interactions are not discussed here. To facilitate our discussion, the $\pi$-interaction in the A-$\pi$(D/T) complexes will be denoted simply as the A-$\pi$(D/T) interaction, where A is a partner atom/molecule/ion. To model the Rg-$\pi$ interaction, Rg is chosen with He and Kr. $CH_4$, $C_2H_6$, and $C_2H_2$ are chosen for the CH-$\pi$ interaction. For the $\pi$-$\pi$(D/T) interaction, we consider benzene, toluene (Tol), and $C_6H_5CN$. For the H-$\pi$(T) interaction, we consider the representative cases of $NH_3$, $H_2O$, HCl, and $CH_3OH$. Notation H$^+$-$\pi$(T) is used for the complex between a non-$\pi$ organic cation and a neutral $\pi$-molecule. For this system, NMe$_4^+$, NH$_4^+$, and NH$_4^+$−w are considered, where "w" denotes a water molecule. These non-$\pi$ organic cations, where the positive charge is more concentrated on the hydrogen atom of the organic molecule cation, are differentiated from the cases of neutral H-$\pi$(T) interactions as seen with the complexes of a neutral $\pi$-system with water, ammonia, alcohols, etc. For the M$^+$-$\pi$ interaction, M is chosen with Cs, K, Na, and Li, while for the M$^{+2}$-$\pi$ interaction, M is chosen with Ca and Mg. These well-studied cation-$\pi$ interactions need to be compared with the $\pi_{\text{cation}}$-$\pi$ interactions which have been commonly observed but hardly investigated. To this end, we have calculated various model complexes involving with these interactions at the same level of theory.

To understand the nature of the $\pi_{\text{cation}}$-$\pi$ interaction, we carry out a detailed and systematic theoretical investigation of diverse intermolecular model systems in which a benzene ring forms the $\pi_{\text{cation}}$-$\pi$ interaction with various positively charged $\pi$ model systems (Figure 2). The first set of models consists of singly charged moieties. Here, the interaction of methyl imidazolium/$N$-methyl-guanidinium with benzene is considered as the representative example for the interaction between the positively charged His/Arg and the neutral aromatic amino moiety (Phe, Tyr, or Trp). The second set of models consists of doubly charged $\pi$-moieties. The third set of models consists of the $\pi_{\text{cation}}$-$\pi$ complexes interacting
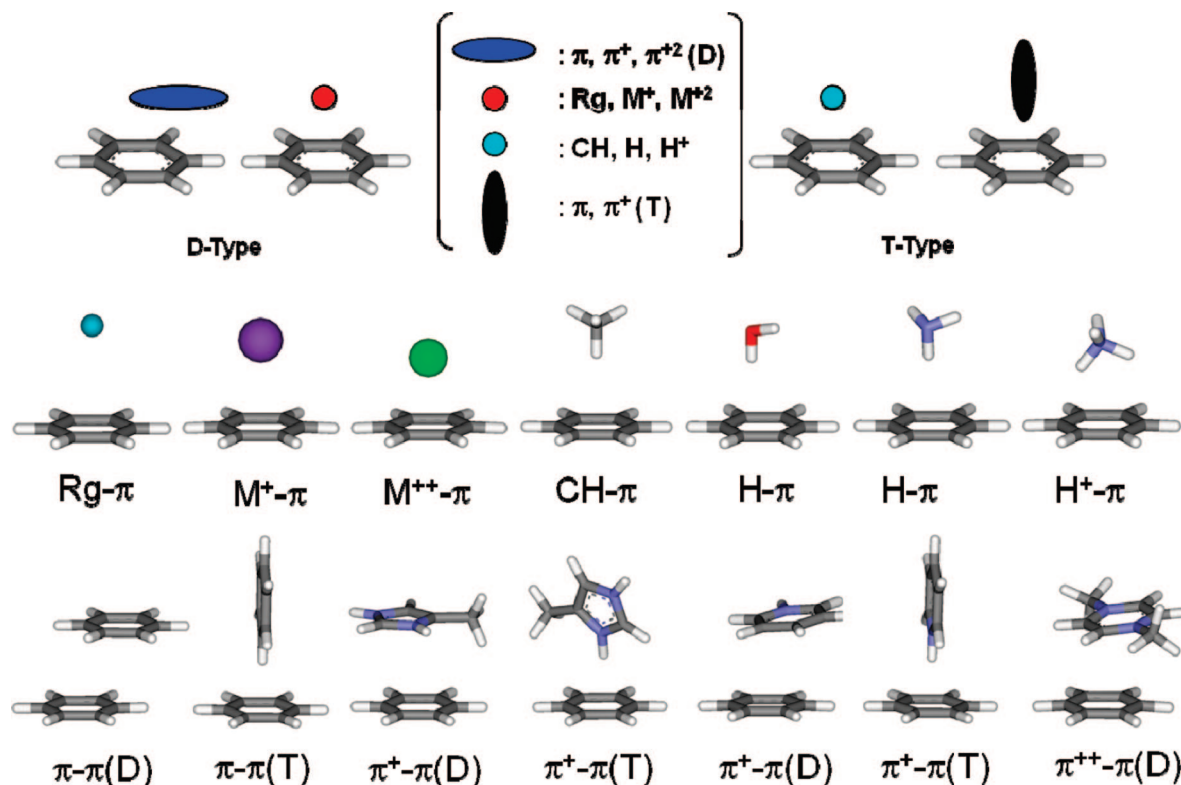
**Figure 1.** Schematic of various types of $\pi$-interaction (See Table 1 for the details of notation).

with water molecules (w) or counteranions ($Cl^-/Br^-$) for the investigation of the effect of solvent molecules and counterions.

**B. Structures and Solvent/Counterion Effects in Terms of Total Interaction Energies.** We discuss the MP2/aVDZ BSSE-corrected geometries and the most reliable CCSD(T)/CBS binding energies (to be denoted as $-E_{tot}$) of various $\pi$-complexes, because the MP2 energies are consistent with the CCSD(T) energies (Table 1).

Figure 3 shows the MP2/aVDZ BSSE-corrected geometries of the $\pi_{cation}$-$\pi$ complexes in the following order. The methyl-guanidinium (ArgH$^+$ moiety; a, a$_t$), methyl imidazolium (HisH$^+$ moiety; b, b$_t$), dimethyl-imidazolium (ImMe$_2^+$; c, c$_t$), and pyridinium (PyH$^+$; d, d$_t$) complexes have both displaced-stacked (D) and T-shaped (T) forms, where "(T)" is explicitly added to the complex name [e.g., ArgH$^+$(T)], while "(D)" is often dropped for brevity's sake unless there is confusion. For the ArgH$^+$/ HisH$^+$/PyH$^+$ complexes, the (N—H)$^+$ group directly points toward the benzene ring plane due to the presence of the positively charged H-atom attached to the N atom, so the most energetically favorable structure is T-shaped. For ImMe$_2^+$, the (C—H)$^+$ directly points to the benzene ring plane. As the H atom in the N—H group is replaced by the methyl group, the 1-methyl pyridinium complex (PyMe$^+$; e), 1,1'-dimethyl- [4,4'] bipyridinium (BPMe$_2^{+2}$; f), and 1,4-dimethyl pyrazinium (PyMe$_2^{+2}$; g) have no option to form T-shaped geometries, so they have the displaced-stacked structures. Furthermore, in the presence of polar solvents (water) or counterions, even the ImMe$_2^+$/PyH$^+$ complexes change to the displaced-stacked forms. Structures h,h'/i,i' and h$_t$/i$_t$ show two different displaced-stacked forms and one T-shaped form

of the ArgH$^+$ moiety interacting with one/two water molecule(s), respectively. In structure h/i, the ArgH$^+$ moiety is significantly displaced from the benzene ring, and the water molecule forms the H-$\pi$ interaction. In structure h'/i', the ArgH$^+$ moiety is stacked with the benzene ring, and the water molecule(s) do not involve in the H-$\pi$ interaction. In the case of HisH$^+$ complex, in the presence of two water molecules, the T-shaped isomer is still more stable than, but nearly isoenergetic to, the displaced-stacked one. Accordingly, both T-shaped and displaced-stacked structures would be compatible depending on the coordination environments. Structures j/k and j$_t$/k$_t$ in Figure 3 show displaced-stacked and T-shaped isomers of the HisH$^+$ moiety interacting with one/two water molecule(s), respectively. Structures l and m show displaced-stacked forms of the pyridinium complexes coordinated by a water molecule and a bromide ion, respectively. Structure n displays the imidazolium complex coordinated by a chloride ion. For these $\pi$-complexes, we find the following trend:

The typical binding energies of the $\pi^+$-$\pi$(D) structures ($\sim$8−11 kcal/mol) and the $\pi^+$-$\pi$(T) structures ($\sim$9−14 kcal/mol) are much larger than the typical H-bonding energy ($\sim$5 kcal/mol for the water dimer),[126] CH-$\pi$ ($\sim$1.5−3 kcal/mol) and H-$\pi$ binding energy ($\sim$2−4 kcal/mol), but smaller than the typical cation-$\pi$ (H$^+$-$\pi$ and M$^+$-$\pi$) binding energy ($\sim$9−23 kcal/mol). In the cases of $\pi^+$-$\pi$ complexes, the most stable structure in the presence of one or two water molecules is often topologically different from that in the gas phase. However, the conventional cation-$\pi$ complexes (non-$\pi$ organic H$^+$-$\pi$ or metallic M$^+$-$\pi$ complexes) retain their structural forms even in the presence of one or two water molecules coordinated to the cationic species.

**Table 1.** Geometrical Parameters (BSSE-corrected MP2/aVDZ) and Interaction Energies (MP2/CBS and CCSD(T)/CBS) of the $\pi_{cation}$ Model Systems Interacting with a Benzene Molecule, Which Are Compared with the Rg-π, CH-π, H-π, π-π, and Cation-π Interactions Involving with a Benzene Molecule[a]

| type | complex | $\theta$ | $r_v$ ($r_d$) | MP2 | | | CCSD(T) | |
|---|---|---|---|---|---|---|---|---|
| | | | | aVDZ | aVTZ | CBS | aVDZ | CBS |
| Rg-π | He | | 3.46 (0.00) | −0.17 | −0.21 | −0.23 | −0.16 | −0.23 |
| | Kr | | 3.64 (0.00) | −1.43 | −1.84 | −2.02 | −0.87 | −1.47 |
| CH-π(T) | $CH_4$ | | 6.80 (0.00) | −1.52 | −1.68 | −1.74 | −1.21 | −1.43 |
| | $C_2H_6$ | −0.9 | 3.66 (0.26) | −2.42 | −2.69 | −2.81 | −1.85 | −2.23 |
| | $C_2H_2$ | 90 | 3.54 (0.00) | −3.04 | −3.32 | −3.45 | −2.44 | −2.85 |
| H−π(T) | $NH_3$ | | 3.60 (0.30) | −2.24 | −2.48 | −2.57 | −1.93 | −2.26 |
| | $H_2O$ | | 3.45 (0.42) | −2.99 | −3.27 | −3.39 | −2.74 | −3.14 |
| | HCl | | 3.67 (0.00) | −4.21 | −4.61 | −4.77 | −3.37 | −3.93 |
| | $CH_3OH$ | | 3.37 (0.37) | −4.06 | −4.47 | −4.64 | −2.74 | −3.14 |
| π-π(T) | $C_6H_6$ (T) | 90 | 4.93 (0.74) | −3.32 | −3.59 | −3.72 | −2.46 | −2.83 |
| | Tol(T) | 90 | 4.84 (0.95) | −3.84 | −4.13 | −4.27 | −2.88 | −3.31 |
| | $C_6H_5CN$(T) | 90 | 4.91 (0.09) | −5.30 | −5.73 | −5.96 | −4.05 | −4.72 |
| π-π(D) | $C_6H_6$ | 0 | 3.41 (1.55) | −4.29 | −4.71 | −4.93 | −2.06 | −2.61 |
| | Tol | 1.8 | 3.38 (1.57) | −5.42 | −5.82 | −6.03 | −3.40 | −4.00 |
| | $C_6H_5CN$ | 4.2 | 3.42 (1.37) | −6.49 | −7.04 | −7.34 | −3.50 | −4.35 |
| $\pi^+$-π(D) | $ArgH^+$ | 0.0 | 3.46 (1.32) | −10.30 | −9.68 | −9.42 | −9.32 | −8.44 |
| | $HisH^+$ | 0.0 | 3.36 (1.11) | −10.11 | −10.72 | −10.98 | −8.05 | −8.92 |
| | $ImMe_2^+$ | 10.2 | 3.36 (1.33) | −11.99 | −12.71 | −13.01 | −9.98 | −11.01 |
| | $PyH^+$ | 6.5 | 3.36 (1.01) | −10.93 | −11.48 | −11.71 | −8.12 | −8.91 |
| | $PyMe^+$ | 7.6 | 3.36 (1.20) | −11.39 | −12.00 | −12.25 | −8.49 | −9.35 |
| | $ArgH^+$-w | −1.2 | 3.22 (2.80) | −9.46 | −10.00 | −10.23 | −8.34 | −9.11 |
| | $ArgH^+$-w' | 12.5 | 3.45 (1.23) | −9.25 | −9.66 | −9.84 | −8.14 | −8.73 |
| | $ArgH^+$-$w_2$ | −2.6 | 3.17 (2.84) | −8.79 | −9.36 | −9.60 | −7.72 | −8.53 |
| | $ArgH^+$-$w_2'$ | 10.5 | 3.44 (1.26) | −8.23 | −8.66 | −8.85 | −7.15 | −7.77 |
| | $HisH^+$-w | 4.0 | 3.33 (0.16) | −9.65 | −10.18 | −10.40 | −7.61 | −8.36 |
| | $HisH^+$-$w_2$ | 1.2 | 3.31 (0.16) | −8.96 | −9.50 | −9.73 | −6.90 | −7.66 |
| | $ImMe_2^+$-$Cl^-$ | 8.8 | 3.29 (1.44) | −10.64 | −11.39 | −11.71 | −8.02 | −9.09 |
| | $PyH^+$-w | 6.9 | 3.37 (1.47) | −10.24 | −10.83 | −11.07 | −7.93 | −8.76 |
| | $PyH$-$Br^-$ | 8.6 | 3.37 (1.31) | −9.03 | −9.64 | −9.90 | −7.97 | −8.85 |
| $\pi^+$-π(T) | $ArgH^+$(T) | 90 | 3.96 (0.46) | −14.35 | −15.00 | −15.27 | −13.04 | −13.96 |
| | $HisH^+$(T) | 73.6 | 4.14 (0.25) | −14.40 | −15.11 | −15.40 | −12.67 | −13.68 |
| | $ImMe_2^+$ (T) | 86.7 | 4.52 (0.10) | −11.90 | −12.55 | −12.83 | −11.10 | −12.03 |
| | $PyH^+$(T) | 90 | 4.38 (0.00) | −15.82 | −16.60 | −16.93 | −14.03 | −15.14 |
| | $ArgH^+$-w(T) | 89.8 | 3.98 (0.55) | −12.91 | −13.54 | −13.80 | −11.69 | −12.58 |
| | $ArgH^+$-$w_2$(T) | 89.8 | 4.01 (0.56) | −8.72 | −9.35 | −9.62 | −7.61 | −8.50 |
| | $HisH^+$-w(T) | 74.7 | 4.18 (0.25) | −13.15 | −13.81 | −14.09 | −11.56 | −12.49 |
| | $HisH^+$-$w_2$(T) | 76.9 | 4.21 (0.13) | −9.63 | −10.42 | −10.75 | −8.16 | −9.28 |
| $H^+$−π(T) | $Me_4N^+$ | | $4.28^b$ (0.00) | −9.86 | −10.28 | −10.46 | −8.89 | −9.49 |
| | $NH_4^+$ | | 2.94 (0.06) | −18.80 | −20.05 | −20.58 | −19.64 | −21.41 |
| | $NH_4^+$-w | | 2.94 (0.07) | −15.14 | −15.88 | −16.19 | −14.25 | −15.29 |
| $\pi^{++}$-π(D) | $PyMe_2^{+2}$ | 8.8 | 3.16 (1.13) | −25.31 | −26.27 | −26.68 | −20.85 | −22.23 |
| | $BPMe_2^{+2}$ | 6.7 | 3.32 (1.13) | −17.48 | −19.33 | −20.11 | | $-16^c$ |
| $M^+$-π | $Cs^+$ | | 3.24 (0.00) | −15.52 | −14.81 | −14.51 | −14.09 | −13.08 |
| | $>K^+$ | | 2.90 (0.00) | −17.12 | −18.74 | −19.42 | −16.47 | −18.77 |
| | $Na^+$ | | 2.48 (0.00) | −22.33 | −22.80 | −23.00 | −22.28 | −22.95 |
| | $Li^+$ | | 1.92 (0.00) | −35.48 | −37.37 | −38.16 | −35.44 | −38.13 |
| | $K^+$-w | | 2.94 (0.00) | −15.10 | −16.32 | −16.83 | −14.50 | −16.22 |
| | $Na^+$-w | | 2.52 (0.00) | −22.28 | −22.64 | −22.79 | −19.19 | −19.70 |
| | $Li^+$-w | | 1.98 (0.00) | −28.77 | −30.16 | −30.74 | −28.63 | −30.30 |
| $M^{++}$-π | $Ca^{2+}$ | | 2.39 (0.00) | −77.85 | −81.43 | −82.93 | −76.32 | −81.40 |
| | $Mg^{2+}$ | | 1.98 (0.00) | −111.94 | −115.24 | −116.63 | −112.16 | −116.85 |
| | $Ca^{2+}$-w | | 2.44 (0.00) | −66.28 | −68.82 | −69.90 | −64.93 | −68.55 |
| | $Mg^{2+}$-w | | 2.02 (0.00) | −94.30 | −96.57 | −97.53 | −94.48 | −97.71 |

[a] $\theta$: angle (in degrees) tilted from the parallel stacking, $r_v$: vertical stacking distance for ring systems or distance from the heavy atom of non-π systems (or the middle carbon atom in the case of $ArgH^+$) to the benzene ring plane, $r_d$: off-center displacement. Distances in Å; energies in kcal/mol. CCSD(T)/CBS $E_{tot}$'s are obtained by applying the correction term (the difference of the BSSE-corrected interaction energies between MP2/aVDZ and CCSD(T)/aVDZ) to the BSSE-corrected MP2/CBS interaction energies (based on the extrapolation scheme utilizing the basis set error in the electron correlation energy proportional to $N^{-3}$ for the aug-cc-pV$NZ$ basis set (reference [34])). [b] Distance between the nitrogen atom and the benzene centroid. The distance from the carbon atom to the benzene ring plane is 3.38 Å. [c] Roughly estimated from the MP2/CBS estimated interaction energy (−20.11 kcal/mol) [For $PyMe_2^{+2}$, the CCSD(T)/CBS energies is ~4.5 kcal/mol less than the MP2/CBS values].

The T-shaped forms of $ArgH^+$(T), $HisH^+$(T), and $PyH^+$(T) ($-E_{tot}$: 14−15 kcal/mol) are ~5−6 kcal/mol more stable than the corresponding displaced-stacked forms. $ImMe_2^+$(T) is ~1 kcal/mol more stable than the displaced-stacked one. How-

ever, other $\pi^+$-π complex structures favor the displaced-stacked forms. The binding energy is ~8−11 kcal/mol for the $\pi^+$-π interaction of the singly charged systems and ~22 kcal/mol for the $\pi^{+2}$-π interaction of the doubly charged
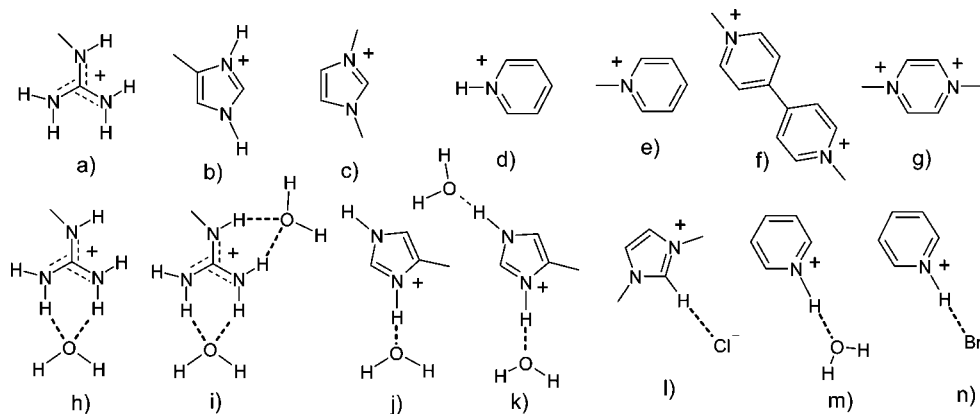
**Figure 2.** Selected positively charged $\pi$-moieties and the associated solvent molecules/counteranions. (a) *N*-methyl-guanidinium (representing the side chain of the protonated arginine), (b) methyl imidazolium (representing the side chain of the protonated histidine), (c) dimethyl imidazolium, (d) pyridinium, (e) 1-methyl pyridinium, (f) 1,1′-dimethyl-[4,4′] bipyridinium, (g) 1,4-dimethyl pyrazinium, (h,i) *N*-methyl-guanidinium with one or two water molecules, (j,k) methyl imidazolium with one or two water molecules, (l) dimethyl imidazolium with a chloride anion, and (m,n) pyridinium with one water molecule or a bromide anion.

systems in a single ring. Doubly charged $BPMe_2^{+2}$ with a positive charge in each of the two rings has the binding energy of ~16 kcal/mol, which is ~7 kcal/mol more than the binding energy of $PyMe^+$ and ~6 kcal/mol less than that of $PyMe_2^{+2}$ (doubly charged on a single ring).

For the $\pi^+$-$\pi$(D) structures, the vertical distance between two stacked rings ($r_v$) is 3.3–3.5 Å for the singly charged systems (except for $ArgH^+$-w/$w_2$(D) which has slightly shorter distances of 3.2 Å due to the large off-center displacement $r_d$), ~3.3 Å for the doubly charged system on two rings, and ~3.2 Å for the doubly charged system on a single ring, which are shorter than the distance (3.41 Å) observed for the neutral benzene-benzene dimer in the displaced-stacked form. It would be noted that the $ArgH^+$ moiety is a weakly $\pi$-conjugated system as compared with aromatic ring systems (such as $HisH^+$, $PyH^+$, and $ImMe_2^+$) discussed here, so the binding energies of the $ArgH^+$(−w/$w_2$) system are slightly smaller than aromatic ring systems.

The solvent and counterion effects play an important role in determining the structures of the $\pi^+$-$\pi$ complexes. For the methyl-guanidium, in the absence of water, the T-shaped $ArgH^+$ moiety is 4.5 kcal/mol more stable than the displaced-stacked one. For the complex with one water molecule, the displaced-stacked $ArgH^+$−w(h) is about 0.5 kcal/mol more stable than the displaced-stacked $ArgH^+$−w(h′), but still 3.5 kcal/mol less stable than the T-shaped $ArgH^+$−w(T)(h$_t$). For the complex with two water molecules, the displaced-stacked $ArgH^+$−w2(i) is about 0.8 kcal/mol more stable than the displaced-stacked $ArgH^+$−w2(i′), and is isoenergetic to or slightly more stable than the T-shaped $ArgH^+$−w2(T)(i$_t$). For the protonated methyl-imidazolium, the T-shaped isomer in the presence of one/two water molecules ($HisH^+$−w(T)(j$_t$)/ $HisH^+$−w2(T)(k$_t$)) is ~4.1/1.7 kcal/mol more stable than the displaced-stacked isomer [$HisH^+$−w(j)/ $HisH^+$−w2(k)]. Either in the presence of both a counteranion (such as an acetate group) and a water molecule or in the presence of more than two coordinating species (water or counteranions or carbonyl oxygen of amide bond, etc.), the T-shaped isomers of $ArgH^+$/$HisH^+$ would eventually be isoenergetic to or slightly less stable than the displaced-stacked isomers.

This result is in good agreement with the previous analysis of proteins and protein−ligand complexes for the interactions of neutral aromatic amino acids with positively charged $\pi$-cloud of protonated arginine/histidine, where the displaced-stacked structure is preferred to the T-shaped structure or otherwise both structures are equally observable.[111−114]

Furthermore, when the T-shaped structures of the $PyH^+$/ $ImMe_2^+$−benzene complexes are optimized in the presence of one water molecule or a counterion, they change to the displaced-stacked structures. Thus, in the presence of polar solvent molecules and counteranions in the vicinity of positively charged $\pi$-systems, the T-shaped forms are no longer stable and so the displaced-stacked forms are favored because the polar solvent molecules and counterions interact with the charged moiety of the charged $\pi$-ring.

The Cambridge structural data analysis (CSD version 5.29, November 2007)[127,128] for the interaction between pyridinium (including substituted and fused ring systems) and benzene (including substituted and fused ring systems) within the centroid-to-centroid intramolecular distance of 5 Å shows that ~90% of the complexes are found to have displaced-stacked structural forms among the total 701 hits. The hydrogen atom in $(N−H)^+$ is in general coordinated to solvent molecules, counteranions, or other partner molecules. We have not found a single example where the hydrogen atom of $(N−H)^+$ directly points to the ring plane of the benzene ring. About 10% of the complexes are found to have angled T-shape structural forms where the hydrogen atom(s) of the C atom(s) of the pyridinium is pointing toward the benzene ring plane. However, the hydrogen atom in $(N−H)^+$ forms a strong hydrogen bond with a solvent molecule, a counteranion, or other partner molecules. Thus, our results are in good agreement with what are observed in the crystal structures.

**C. Energy Components.** Table 2 lists $E_{tot}$ and SAPT energy components of various $\pi$-model systems, and these average values for various types of $\pi$-interactions are listed in Table 3. Figure 4a shows the 3-dimensional (3D) plot of $E_{tot}$ as the function of $E_{exch*}$ and $E_{attr}$ and Figure 4b shows the 3D plot of $E_{tot}$ as the function of $E_{es*}$ and $E_{ind**}$. Figure
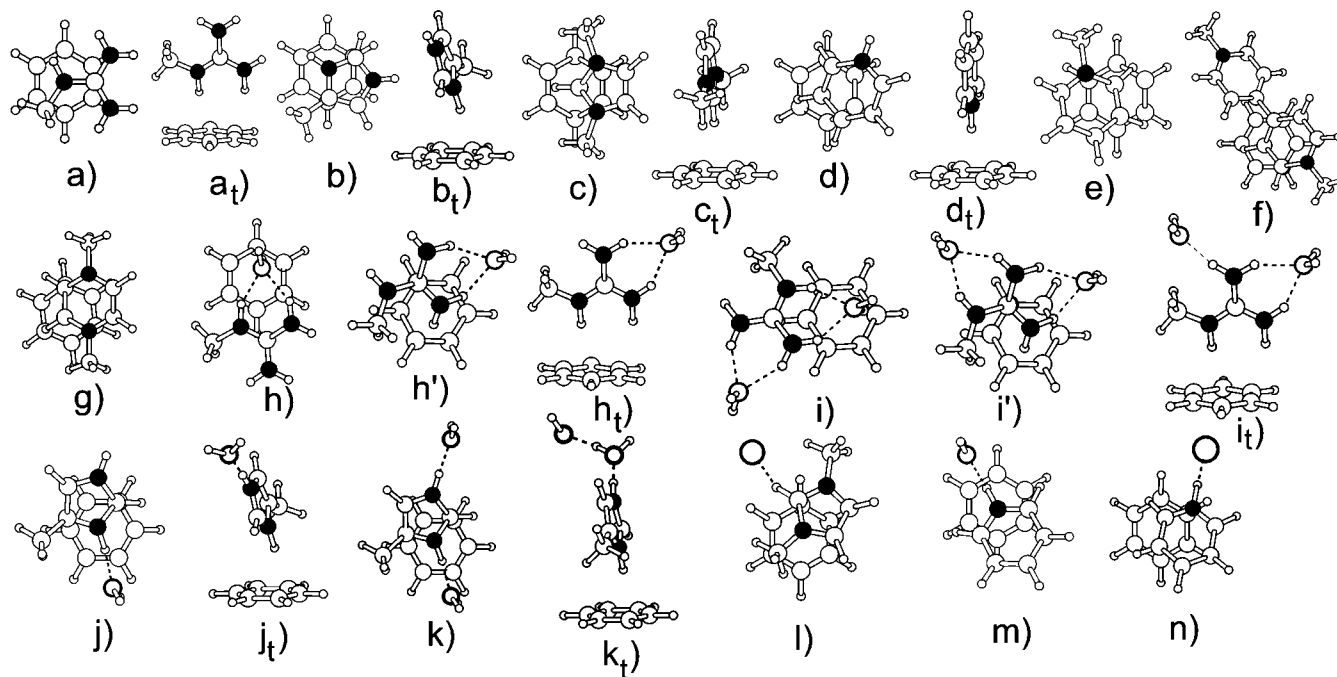
**Figure 3.** Calculated geometries (BSSE-corrected MP2/aug-cc-pVDZ) of model complex systems whose positively charged aromatic ring interacts with a neutral aromatic benzene ring: displaced stacked (D) and T-shaped (T) forms of *N*-methyl-guanidinium complexes (ArgH$^+$(D), ArgH$^+$(T)) (a$_t$,a); displaced stacked and T-shaped forms of the methyl imidazolium complexes (HisH$^+$(D), HisH$^+$(T)) (b$_t$,b); dimethyl imidazolium complex in displaced-stacked and T-shape forms (ImMe$_2^+$(D), ImMe$_2^+$(T)) (c$_t$,c); displaced stacked and T-shaped forms of the pyridinium complexes (PyH$^+$(D), PyH$^+$(T)) (d$_t$,d); 1-methyl pyridinium complex (PyMe$^+$) (e); the 1,1'-dimethyl-[4,4'] bipyridinium complex (BPMe$_2^{+2}$) (f); 1,4-dimethyl pyrazinium complex (PyMe$_2^{+2}$) (g); *N*-methyl-guanidinium complexes coordinated by one (w) and two water (w2) molecules in two displaced-stacked and T-shaped forms (h, h', h$_t$ and i, i', i$_t$,); methyl imidazolium complexes coordinated by one (w) and two water (w2) molecules in displaced-stacked and T-shaped forms (j, j$_t$, and k, k$_t$); dimethyl imidazolium complex coordinated by chloride (ImMe$_2^+$–Cl$^-$) (l); and pyridinium complexes coordinated by water and bromide (PyH$^+$-w, PyH$^+$-Br$^-$) (m, n). In BPMe$_2^{+2}$, one ring is twisted by ∼37 ° with respect to the other ring interacting with the neutral benzene ring. The other structure that both rings are planar is ∼2 kcal/mol less stable. Structures h' and i' are slightly less stable than structures h and i, respectively.

4c plots the correlation of $E_{\text{tot}}$ with (i) $E_{\text{es}*}$, (ii) $E_{\text{ind}**}$, (iii) $E_{\text{es,ind}}$ ($E_{\text{es,ind}} = E_{\text{es}*} + E_{\text{ind}**}$), and (iv) $E_{\text{disp,exch}}$ ($E_{\text{disp,exch}} = E_{\text{disp}**} + E_{\text{exch}*}$). The $E_{\text{es}*}$ (square of correlation factor, $R^2 = 0.921$), $E_{\text{ind}**}$ ($R^2 = 0.993$), $E_{\text{es,ind}}$ ($R^2 = 0.997$), and $E_{\text{disp,exch}}$ ($R^2 = 0.927$) show correlations with $E_{\text{tot}}$, while $E_{\text{disp}**}$ and $E_{\text{exch}*}$ do not show good correlations with $E_{\text{tot}}$. Hence, $E_{\text{tot}}$ shows a good correlation with $E_{\text{ind}**}$ and in particular, $E_{\text{es,ind}}$. In the $E_{\text{tot}}$ vs $E_{\text{es}*}$ regression, the quadratic polynomial regression of $E_{\text{es}*}$ with respect to $E_{\text{tot}}$ drastically improves the correlation ($R^2 = 0.980$ for $E_{\text{es}*}$). This indicates the importance of the square terms of $E_{\text{es}*}$, where $E_{\text{es}*}$ is related to site charges, which implicitly reflects the induction term proportional to the square of the electric field correlated to the site charges. Hence, the $E_{\text{tot}}$ vs $E_{\text{es,ind}}$ linear regression results in an excellent correlation ($R^2 = 0.997$). This indicates that the difference in $E_{\text{tot}}$ between different types of $\pi$-interaction can be reasonably explained by $E_{\text{es,ind}}$. However, it does not mean that $E_{\text{es,ind}}$ can explain small differences between same types of $\pi$-interaction such as $\pi$-$\pi$-(D), since $E_{\text{es,ind}}$ alone cannot properly distinguish small energy difference in $E_{\text{tot}}$ due to substitution in aromatic ring.[43] $E_{\text{disp}**}$ and $E_{\text{exch}*}$ independently show very poor correlations with $E_{\text{tot}}$ (Figure 4c-iv), while $E_{\text{disp,exch}}$ shows an anticorrelation with $E_{\text{tot}}$. Overall, the $E_{\text{es}*}$ component shares a large portion of $E_{\text{tot}}$, but its variation depending on the types of $\pi$-interaction is not substantial. However, the $E_{\text{ind}**}$ component changes

drastically depending on the types of $\pi$-interaction. In this regard, $E_{\text{ind}**}$ is the crucial energy component to differentiate different types of $\pi$-interaction, while other components also play significant roles in differentiating them. The detailed analysis of Tables 2 and 3 as well as Figure 4 is given in the Supporting Information. Here, we discuss only the main essence of the findings in the next paragraphs.

In going from the Rg-$\pi$ complexes to the M$^{+2}$-$\pi$ complexes, the increasing order in the values of $-E_{\text{es}*}$ or $-E_{\text{ind}**}$ is not correlated with the increasing/decreasing order in the values of $-E_{\text{disp}**}$ or $E_{\text{exch}*}$. A general observation from the above analysis is that $-E_{\text{es}*}$ and $-E_{\text{ind}**}$ are the smallest in the Rg-$\pi$ complexes, followed by the CH-$\pi$, $\pi$-$\pi$, and H-$\pi$ complexes, while they are large in the $\pi^{+2}$-$\pi$(D) and M$^{+2}$-$\pi$ complexes. $-E_{\text{es}*}$ is larger than $-E_{\text{ind}*}$ in all the M$^{+2}$-$\pi$ complexes with the exception of the Li$^+$ and Li$^+$–w complexes. For the M$^+$-$\pi$ interaction, there is a large variation in $-E_{\text{ind}**}$ (5–30 kcal/mol) because the Cs$^+$/Li$^+$ ion is at a very long/short distance from the benzene molecule. In all of the charged $\pi$-complexes, the electrostatic energy is important, and so is the induction energy except for the $\pi^+$-$\pi$(D) complexes.

The $\pi^+$-$\pi$(D), $\pi$-$\pi$(D), and $\pi^{+2}$-$\pi$(D) complexes have large dispersion energy (E$_{\text{disp}**}$, ∼9–13 kcal/mol), while the M$^+$-$\pi$ complexes have small dispersion energy (∼0.6–6 kcal/mol).

**Table 2.** Interaction Energies ($E_{tot}$: CCSD(T)/CBS), Energy Components ($E_{es^*}$, $E_{ind^{**}}$, $E_{disp^{**}}$, $E_{exch^*}$; $E_{attr} = E_{es^*} + E_{ind^{**}} + E_{disp^{**}}$) at the SAPT(MP2)/6-31+G* level or a VDZ$^+$ level, and Fractional Values of Energy Components Reported in Percentages [$f_{es} = E_{es^*}/E_{attr}$, $f_{ind} = E_{ind^{**}}/E_{attr}$, $f_{disp^{**}} = E_{disp^{**}}/E_{attr}$, $f_{exch} = -E_{exch^*}/E_{attr}$, $f_{es,ind} = (E_{es^*} + E_{ind^{**}})/(E_{attr} - E_{exch^*})$, $f_{disp^{**}} = E_{disp^*}/(E_{attr} - E_{exch^*})$, $f_{exch^*} = -E_{exch^*}/(E_{attr} - E_{exch^*})$] of the $\pi$-Model Systems Interacting with a Benzene Molecule$^a$

| type | complex | $E_{tot}$ | $E_{es^*}$ | $E_{ind^{**}}$ | $E_{disp^{**}}$ | $E_{exch^*}$ | $f_{es}$ | $f_{ind}$ | $f_{disp}$ | $f_{exch}$ | $f'_{es,ind}$ | $f'_{disp}$ | $f'_{exch}$ |
|---|---|---|---|---|---|---|---|---|---|---|---|---|---|
| Rg-$\pi$ | He | −0.23 | −0.04 | −0.02 | −0.32 | 0.15 | 9.9 | 5.9 | 84.1 | 40.5 | 11.3 | 59.9 | 28.8 |
| | Kr | −1.47 | −0.91 | −0.17 | −2.67 | 2.28 | 24.2 | 4.4 | 71.3 | 60.8 | 17.8 | 44.3 | 37.8 |
| CH-$\pi$(T) | CH$_4$ | −1.43 | −0.91 | −0.25 | −2.46 | 2.19 | 25.1 | 6.9 | 68.0 | 60.5 | 19.9 | 42.4 | 37.7 |
| | C$_2$H$_6$ | −2.23 | −1.53 | −0.39 | −4.11 | 3.80 | 25.3 | 6.5 | 68.2 | 63.0 | 19.5 | 41.8 | 38.7 |
| | C$_2$H$_2$ | −2.85 | −2.23 | −0.83 | −3.10 | 3.32 | 36.2 | 13.5 | 50.3 | 53.8 | 32.3 | 32.7 | 35.0 |
| H−$\pi$(T) | NH$_3$ | −2.26 | −1.78 | −0.43 | −2.57 | 2.52 | 37.3 | 8.9 | 53.8 | 52.6 | 30.3 | 35.3 | 34.5 |
| | H$_2$O | −3.34 | −2.73 | −0.79 | −2.81 | 2.99 | 43.2 | 12.5 | 44.4 | 47.3 | 37.8 | 30.1 | 32.1 |
| | HCl | −3.93 | −3.41 | −1.33 | −3.73 | 4.53 | 40.3 | 15.7 | 44.0 | 53.5 | 36.5 | 28.7 | 34.9 |
| | CH$_3$OH | −4.11 | −3.40 | −1.06 | −4.65 | 5.00 | 37.3 | 11.7 | 51.0 | 54.9 | 31.6 | 32.9 | 35.4 |
| $\pi$-$\pi$(T) | C$_6$H$_6$ (T) | −2.83 | −2.11 | −0.53 | −4.17 | 3.98 | 31.0 | 7.8 | 61.2 | 58.5 | 24.5 | 38.6 | 36.9 |
| | Tol(T) | −3.31 | −2.35 | −0.59 | −5.08 | 4.71 | 29.3 | 7.4 | 63.3 | 58.7 | 23.1 | 39.9 | 37.0 |
| | C$_6$H$_5$CN(T) | −4.72 | −4.24 | −1.28 | −6.10 | 6.91 | 36.5 | 11.0 | 52.5 | 59.5 | 29.8 | 32.9 | 37.3 |
| $\pi$-$\pi$(D) | C$_6$H$_6$ | −2.61 | −2.58 | −0.84 | −7.57 | 8.38 | 23.5 | 7.6 | 68.9 | 76.3 | 17.6 | 39.1 | 43.3 |
| | Tol | −4.00 | −3.26 | −0.98 | −9.66 | 9.90 | 23.5 | 7.0 | 69.5 | 71.2 | 17.8 | 40.6 | 41.6 |
| | C$_6$H$_5$CN | −4.35 | −5.02 | −1.08 | −9.61 | 11.36 | 32.0 | 6.9 | 61.2 | 72.3 | 22.5 | 35.5 | 42.0 |
| $\pi^+$-$\pi$(D) | ArgH$^+$ | −8.44 | −5.99 | −2.38 | −7.49 | 7.42 | 37.8 | 15.0 | 47.2 | 46.8 | 36.0 | 32.2 | 31.9 |
| | HisH$^+$ | −8.92 | −7.36 | −2.89 | −8.86 | 10.86 | 38.5 | 15.1 | 46.4 | 56.8 | 34.2 | 29.6 | 36.2 |
| | ImMe$_2^+$ | −11.01 | −8.61 | −3.19 | −10.57 | 11.36 | 38.5 | 14.2 | 47.3 | 50.8 | 35.0 | 31.3 | 33.7 |
| | PyH$^+$ | −8.91 | −8.68 | −3.76 | −9.09 | 12.61 | 40.3 | 17.5 | 42.2 | 58.6 | 36.4 | 26.6 | 36.9 |
| | PyMe$^+$ | −9.35 | −8.64 | −3.57 | −10.02 | 12.87 | 38.9 | 16.1 | 45.1 | 57.9 | 34.8 | 28.6 | 36.7 |
| | ArgH$^+$−w | −9.11 | −7.89 | −3.90 | −7.10 | 9.78 | 41.8 | 20.6 | 37.6 | 51.8 | 41.1 | 24.8 | 34.1 |
| | ArgH$^+$−w′ | −8.73 | −7.94 | −3.40 | −7.31 | 9.91 | 42.6 | 18.2 | 39.2 | 53.1 | 39.7 | 25.6 | 34.7 |
| | ArgH$^+$−w$_2$ | −8.53 | −7.45 | −3.45 | −7.26 | 9.64 | 41.0 | 19.0 | 40.0 | 53.1 | 39.2 | 26.1 | 34.7 |
| | ArgH$^+$−w$_2$′ | −7.77 | −7.18 | −2.76 | −7.36 | 9.53 | 41.5 | 16.0 | 42.5 | 55.1 | 37.0 | 27.4 | 35.5 |
| | HisH$^+$−w | −8.36 | −7.38 | −2.80 | −9.04 | 10.87 | 38.4 | 14.6 | 47.1 | 56.5 | 33.8 | 30.1 | 36.1 |
| | HisH$^+$−w$_2$ | −7.66 | −6.88 | −2.43 | −9.15 | 10.79 | 37.3 | 13.1 | 49.6 | 58.5 | 31.8 | 31.3 | 36.9 |
| | ImMe$_2^+$-Cl$^-$ | −9.09 | −11.08 | −3.43 | −11.53 | 16.94 | 42.6 | 13.2 | 44.3 | 65.1 | 33.8 | 26.8 | 39.4 |
| | PyH$^+$−w | −8.76 | −7.86 | −3.02 | −9.28 | 11.41 | 39.0 | 15.0 | 46.0 | 56.6 | 34.5 | 29.4 | 36.1 |
| | PyH-Br$^-$ | −8.85 | −9.17 | −2.47 | −11.94 | 14.73 | 38.9 | 10.5 | 50.6 | 62.5 | 30.4 | 31.2 | 38.5 |
| $\pi^+$-$\pi$(T) | ArgH$^+$(T) | −13.96 | −10.88 | −7.40 | −7.61 | 11.92 | 42.0 | 28.6 | 29.4 | 46.0 | 48.4 | 20.1 | 31.5 |
| | HisH$^+$(T) | −13.68 | −10.22 | −7.22 | −7.86 | 11.62 | 40.4 | 28.5 | 31.1 | 45.9 | 47.2 | 21.3 | 31.5 |
| | ImMe$_2^+$ (T) | −12.03 | −8.34 | −5.06 | −7.79 | 9.16 | 39.3 | 23.9 | 36.8 | 43.2 | 44.1 | 25.7 | 30.2 |
| | PyH$^+$(T) | −15.14 | −10.98 | −7.74 | −8.06 | 11.64 | 41.0 | 28.9 | 30.1 | 43.5 | 48.7 | 21.0 | 30.3 |
| | ArgH$^+$−w(T) | −12.58 | −9.86 | −6.16 | −7.47 | 10.90 | 42.0 | 26.2 | 31.8 | 46.4 | 46.6 | 21.7 | 31.7 |
| | ArgH$^+$-w$_2$(T) | −8.50 | −9.18 | −5.39 | −4.22 | 10.30 | 48.8 | 28.7 | 22.5 | 54.8 | 50.1 | 14.5 | 35.4 |
| | HisH$^+$−w(T) | −12.49 | −9.39 | −6.17 | −7.59 | 10.66 | 40.6 | 26.6 | 32.8 | 46.0 | 46.0 | 22.4 | 31.5 |
| | HisH$^+$−w$_2$(T) | −9.28 | −8.94 | −5.61 | −4.76 | 10.02 | 46.3 | 29.0 | 24.6 | 51.9 | 49.6 | 16.2 | 34.2 |
| H$^+$-$\pi$(T) | Me$_4$N$^+$ | −9.49 | −7.33 | −4.04 | −6.37 | 8.25 | 41.3 | 22.8 | 35.9 | 46.5 | 43.7 | 24.5 | 31.7 |
| | NH$_4^+$ | −21.20 | −13.27 | −14.08 | −6.85 | 13.00 | 38.8 | 41.2 | 20.0 | 38.0 | 57.9 | 14.5 | 27.5 |
| | NH$_4^+$−w | −15.29 | −12.00 | −10.57 | −5.97 | 13.24 | 42.0 | 37.0 | 20.9 | 46.4 | 54.0 | 14.3 | 31.7 |
| $\pi^{++}$-$\pi$(D) | PyMe$_2^{+2}$ | −22.23 | −17.56 | −14.16 | −13.15 | 22.64 | 39.1 | 31.6 | 29.3 | 50.5 | 47.0 | 19.5 | 33.5 |
| M$^+$-$\pi$ | Cs$^+$ | −13.08 | −12.97 | −5.62 | −5.63 | 11.13 | 53.5 | 23.2 | 23.3 | 46.0 | 52.6 | 15.9 | 31.5 |
| | K$^+$ | −18.77 | −13.59 | −9.98 | −3.57 | 8.36 | 50.1 | 36.8 | 13.1 | 30.8 | 66.4 | 10.1 | 23.6 |
| | Na$^+$ | −22.95 | −15.64 | −13.84 | −0.59 | 6.81 | 52.0 | 46.0 | 2.0 | 22.7 | 79.9 | 1.6 | 18.5 |
| | Li$^+$ | −38.13 | −17.84 | −29.97 | −0.59 | 10.28 | 36.9 | 61.9 | 1.2 | 21.2 | 81.5 | 1.0 | 17.5 |
| | K$^+$−w | −16.22 | −12.28 | −8.18 | −3.27 | 7.51 | 51.8 | 34.5 | 13.8 | 31.6 | 65.5 | 10.5 | 24.0 |
| | Na$^+$−w | −19.70 | −13.93 | −11.19 | −0.76 | 6.00 | 53.8 | 43.2 | 2.9 | 23.2 | 78.8 | 2.4 | 18.8 |
| | Li$^+$−w1 | −30.60 | −15.29 | −22.23 | −1.26 | 8.18 | 39.4 | 57.3 | 3.3 | 21.1 | 79.9 | 2.7 | 17.4 |
| M$^{++}$-$\pi$ | Ca$^{2+}$ | −81.40 | −36.17 | −69.62 | −6.28 | 30.67 | 32.3 | 62.1 | 5.6 | 27.4 | 74.1 | 4.4 | 21.5 |
| | Mg$^{2+}$ | −116.85 | −40.11 | −102.82 | −0.39 | 26.47 | 28.0 | 71.7 | 0.3 | 18.5 | 84.2 | 0.2 | 15.6 |
| | Ca$^{2+}$−w | −68.55 | −33.26 | −57.35 | −5.24 | 27.29 | 34.7 | 59.8 | 5.5 | 28.5 | 73.6 | 4.3 | 22.2 |
| | Mg$^{2+}$−w | −97.71 | −36.32 | −84.20 | −1.22 | 24.03 | 29.8 | 69.2 | 1.0 | 19.7 | 82.7 | 0.8 | 16.5 |

$^a$ SAPT(MP2)/6−31+G* is used for the energy component calculations of $\pi$-$\pi$(D), $\pi$-$\pi$(T), $\pi^+$-$\pi$(D), $\pi^+$-$\pi$(T), $\pi^{+2}$-$\pi$(D), M$^+$-$\pi$, and M$^{+2}$-$\pi$ complexes, while SAPT(MP2)/aVDZ′ is used for Rg-$\pi$, CH-$\pi$, H-$\pi$(T), and H$^+$-$\pi$(T) complexes, as the total energies were highly underestimated for these complexes at the SAPT(MP2)/6−31+G* level. The $E_{es^*}$, $E_{ind^{**}}$, $E_{disp^{**}}$, and $E_{exch^*}$ values at the SAPT(MP2)/aVDZ$^\dagger$ level are, respectively: −10.22, −8.18, −8.57, 11.83 for PyH$^+$(T); −8.44, −4.00, −9.44, 13.00 for PyH$^+$(D); −8.34, −3.74, −10.31, and 13.07 for PyMe$^+$. These values are consistent with the SAPT(MP2)/6−31+G* results, as in the table. While the base set dependency of $E_{es^*}$ and $E_{exch^*}$ is not significant, $E_{disp^*}$ and $E_{ind^*}$ depend on the basis set. Thus, the realistic $E_{disp^{**}}$ and $E_{ind^{**}}$ are obtained as described in computational details and Supporting Information.

The Rg-$\pi$, CH-$\pi$(T), and H-$\pi$(T) complexes have small exchange energy, while the $\pi^{+2}$-$\pi$(D) and M$^{+2}$-$\pi$ complexes have very large exchange energy. Given that the dispersion energy depends on the size of a partner molecule or the total number of electrons or the sum of atomic numbers, the values of $-E_{disp^{**}}$ of the H-$\pi$(T) interactions composed of only small

species in this study are much smaller than those of other types of $\pi$-interaction. If similar sizes are considered, then the CH-$\pi$(T) and H-$\pi$(T) interactions would be more or less equivalent in $-E_{disp^{**}}$ to the $\pi$-$\pi$(T) interaction.

In the Rg-$\pi$ complex (Rg = He, Kr), $-E_{disp^{**}}$ (0.32−2.7 kcal/mol) is partly canceled by $E_{exch^*}$, gaining only a small

***Table 3.*** Average Interaction Energies ($E_{tot}$: CCSD(T)/CBS), Energy Components (SAPT(MP2)/6-31+G*), and Energy Component Percentages for the Various Types of $\pi$-Interactions, Which Are Ordered in Terms of Increasing Induction Energy Component Percentage $f_{ind}$

| | $E_{tot}$ | $E_{es*}$ | $E_{ind**}$ | $E_{disp**}$ | $E_{exch*}$ | $f_{es}$ | $f_{ind}$ | $f_{disp}$ | $f_{es,ind}$ | $f_{disp}$ | $f_{exch}$ |
|---|---|---|---|---|---|---|---|---|---|---|---|
| Rg-$\pi$ | −0.8 | −0.5 | −0.1 | −1.5 | 1.2 | 17.1 | 5.2 | 77.7 | 14.6 | 52.1 | 33.3 |
| $\pi$-$\pi$ (D) | −3.7 | −3.6 | −1.0 | −8.9 | 9.9 | 26.3 | 7.2 | 66.5 | 19.3 | 38.4 | 42.3 |
| $\pi$ -$\pi$(T) | −3.6 | −2.9 | −0.8 | −5.1 | 5.2 | 32.3 | 8.7 | 59.0 | 25.8 | 37.2 | 37.1 |
| CH-$\pi$(T) | −2.2 | −1.6 | −0.5 | −3.2 | 3.1 | 28.9 | 9.0 | 62.1 | 23.9 | 39.0 | 37.1 |
| H-$\pi$ (T) | −3.4 | −2.8 | −0.9 | −3.4 | 3.8 | 39.5 | 12.2 | 48.3 | 34.0 | 31.7 | 34.2 |
| $\pi^+$-$\pi$ (D) | −8.8 | −8.0 | −3.1 | −9.0 | 11.3 | 39.8 | 15.6 | 44.6 | 35.5 | 28.6 | 35.8 |
| $\pi^+$-$\pi$(T) | −12.2 | −9.7 | −6.3 | −6.9 | 10.8 | 42.6 | 27.6 | 29.9 | 47.6 | 20.4 | 32.0 |
| $\pi^{++}$-$\pi$(D) | −22.2 | −17.6 | −14.2 | −13.1 | 22.6 | 39.1 | 31.6 | 29.3 | 47.0 | 19.5 | 33.5 |
| H$^+$-$\pi$(T) | −15.3 | −10.9 | −9.6 | −6.4 | 11.5 | 40.7 | 33.7 | 25.6 | 51.9 | 17.8 | 30.3 |
| M$^+$-$\pi$ | −22.8 | −14.5 | −14.4 | −2.2 | 8.3 | 48.2 | 43.3 | 8.5 | 72.1 | 6.3 | 21.6 |
| M$^{++}$-$\pi$ | −91.1 | −36.5 | −78.5 | −3.3 | 27.1 | 31.2 | 65.7 | 3.1 | 78.6 | 2.4 | 18.9 |

amount of binding energy. However, as the electron density in the space between benzene and He/Kr is redistributed outside the benzene−Kr complex (while it is slightly more distributed outside benzene), there is small $-E_{es*}$ due to small charge transfer from the benzene ring to the Rg (natural bond orbital charge of −0.003 au for Kr at the CCSDT(T)/aVDZ level) as well as small polarization-driven $-E_{ind**}$, resulting in a substantial binding energy contribution in the small total binding energy. In the CH-$\pi$ complexes, $-E_{disp**}$ is larger than $-E_{es*}$, and $-E_{ind**}$ is relatively small.

The $\pi$-$\pi$(D) complexes have larger $-E_{disp**}$ ($\sim$8−10 kcal/mol) than the $\pi$-$\pi$(T) complexes ($\sim$4−6 kcal/mol), which are larger than corresponding $-E_{es}$ ($\sim$2−5 kcal/mol) and $-E_{ind*}$ ($\sim$0.5−1 kcal/mol). However, the H-$\pi$(T) complexes tend to have smaller $-E_{disp**}$ (2.5−4.6 kcal/mol) than the $\pi$-$\pi$(T) complexes in this study. However, given that the partner molecules in the H-$\pi$(T) complexes are smaller than those in $\pi$-$\pi$(T) complexes, there would be no significant differences in $E_{disp**}$ between H-$\pi$(T) and $\pi$-$\pi$(T) complexes.

In the $\pi^+$-$\pi$(D) complexes, $-E_{disp**}$ ($\sim$7−12 kcal/mol) is only slightly larger than $-E_{es*}$, while $-E_{ind**}$ is small and $E_{exch*}$ is relatively large. These are contrasted to the $\pi^+$-$\pi$(T) complexes, where $-E_{es*}$ ($\sim$8−11 kcal/mol) is larger than $-E_{disp**}$. In this regard, the H$^+$-$\pi$(T) complexes are similar to those of $\pi^+$-$\pi$(T) complexes. The $-E_{es*}$ of small organic cations (NH$_4^+$ and NH$_4^+$−w) are nearly similar to $-E_{ind**}$, while for bigger organic cations (Me$_4$N$^+$) $-E_{es*}$ is larger than $-E_{ind**}$. In the $\pi^+$-$\pi$(T)/ H$^+$-$\pi$(T) complexes, $-E_{exch*}$ and $-E_{ind**}$ are much larger than those in the $\pi$-$\pi$(D), $\pi$-$\pi$(T) and $\pi^+$-$\pi$(D) complexes. Alternatively, in the $\pi^{++}$-$\pi$(D) complex of PyMe$_2^{+2}$, the $-E_{es*}$ (18 kcal/mol) is larger than $-E_{ind**}$ and $-E_{disp**}$, but smaller than $E_{exch*}$.

In the M$^+$-$\pi$ complexes, $-E_{es*}$ ($\sim$12−16 kcal/mol) is larger than $-E_{ind**}$ excluding the Li$^+$ and Li$^+$−w complexes where $-E_{es*}$ is smaller than $-E_{ind**}$. These are contrasted to the M$^{++}$-$\pi$ complexes where $-E_{ind**}$ ($\sim$57−102 kcal/mol) is larger than $-E_{es*}$. In both M$^+$-$\pi$ and M$^{+2}$-$\pi$ complexes, $-E_{disp**}$ is much smaller than $E_{exch*}$. For the M$^{+2}$-$\pi$ complexes, the magnitude of the sum of the attractive energy components ($-E_{attr}$) is much larger than $E_{exch*}$, hence the binding energy is the largest among the $\pi$-complexes studied here.

One may note at this point that the $\pi$-$\pi$ interaction has large dispersion energy, the cation-$\pi$ interaction has large electrostatic and induction energies, and the $\pi^+$-$\pi$ interaction has large dispersion and electrostatic energies. Since the total energies vary significantly depending on the types of $\pi$-complexes, the degree of contribution of these energy components to the total binding energy is another way to analyze different types of $\pi$-complexes. Thus, to more clearly understand the similarities and differences between these important $\pi$ interactions, we look into the percentage contributions from each of the attractive and repulsive energy components using the ternary diagram analysis.

**D. Ternary Diagram Analysis.** Since each $\pi$-interaction is represented by five components ($E_{tot}$, $E_{es}$, $E_{ind*}$, $E_{disp**}$, and $E_{exch*}$), a clustering scheme in multidimensional spaces is utilized to differentiate different types of $\pi$-interaction. Due to the complexity involved with the multidimensional clustering techniques, it would be useful to exploit three component ternary diagrams which are popular for the interpretation of the phase transition in physical chemistry.[129] Figure 5 shows some of selected ternary diagrams drawn using the combination of variously selected energy components.

In Figure 5a, the ternary diagram using the attractive energy components ($E_{es*}$, $E_{ind**}$, $E_{disp**}$) shows the percentage of $E_{es*}/E_{ind**}/E_{disp**}$, i.e., $f_{es}/f_{ind}/f_{disp}$ (in %) in the total attractive interaction energy for different types of $\pi$-interaction. The average percentages of $f_{es}/f_{ind}/f_{disp}$ are $\sim$17/**5**/78% for Rg-$\pi$, $\sim$26/**7**/67% for $\pi$-$\pi$(D), $\sim$32/**9**/59% for $\pi$-$\pi$(T), $\sim$29/**9**/62% for CH-$\pi$, $\sim$40/**12**/48% for H-$\pi$, $\sim$40/**16**/44% for $\pi^+$-$\pi$(D), $\sim$43/**27**/30% for $\pi^+$-$\pi$(T), $\sim$39/**31**/30% for $\pi^{+2}$-$\pi$(D), $\sim$41/**34**/25% for H$^+$-$\pi$(T), $\sim$48/**43**/9% for M$^+$-$\pi$, and $\sim$31/**66**/3% for M$^{+2}$-$\pi$ (Table 3), which are listed in the increasing order of the average induction energy percentage. The main points that could be drawn from figure 5a (Table 2) are highlighted below (the detailed analysis is in Supporting Information).

The variation of $f_{es}$ between different types of $\pi$-interaction is rather small as compared to the variations of $f_{ind}$. Whereas, the $f_{disp}$ and $f_{exch}$ are almost in the reverse order of $f_{ind}$. The dispersion energy is the highly dominant component in the Rg-$\pi$ ($\sim$78%), CH-$\pi$ ($\sim$62%), and $\pi$-$\pi$(D) ($\sim$67%) complexes and the dominant component ($\sim$59%) in the $\pi$-$\pi$(T) complexes, whereas all their induction components are very small (5−9%). The $f_{exch}$ increases with increasing contacting area between benzene and the partner molecule and with increasing charge density in the contacting area. More
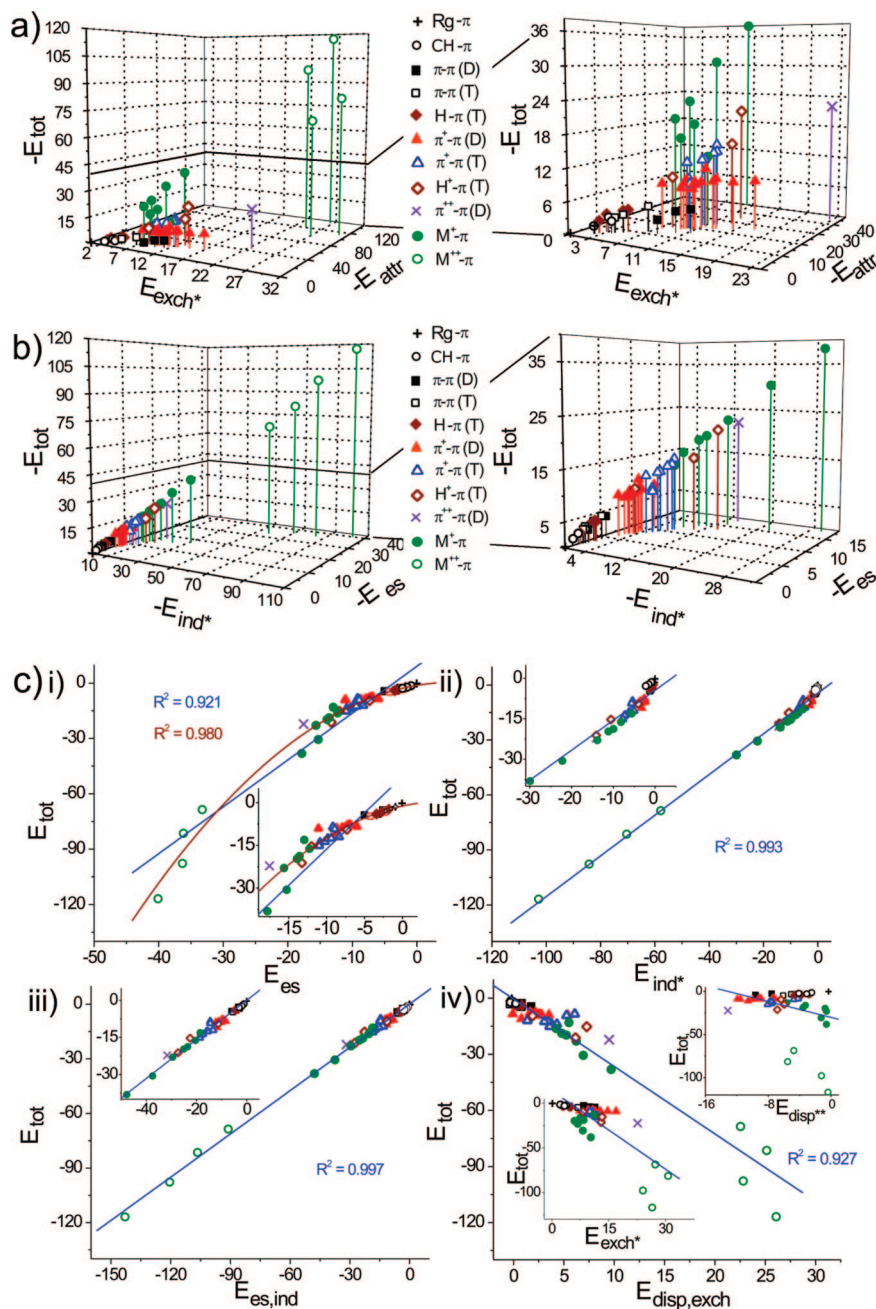
**Figure 4.** 3D-plots of (a) $-E_{tot}$ as the function of $E_{exch^*}$ and $-E_{attr}(E_{attr} = E_{es^*} + E_{ind^{**}} + E_{disp^{**}})$ and (b) $-E_{tot^*}$ as the function of $-E_{ind^{**}}$ and $-E_{es^*}$ for the Rg-$\pi$, CH-$\pi$(T), $\pi$-$\pi$(D), $\pi$-$\pi$(T), H-$\pi$(T), $\pi^+$-$\pi$(D), $\pi^+$-$\pi$(T), H$^+$-$\pi$(T), $\pi^{+2}$-$\pi$(D), M$^+$-$\pi$, and M$^{+2}$-$\pi$ interactions which are described in Tables 1 and 2. (c) Linear or multiple linear polynomial regression curves between (i) $E_{tot}$ and $E_{es^*}$, (ii) $E_{tot}$ and $E_{ind^{**}}$, (iii) $E_{tot}$ and $E_{es,ind}$ ($= E_{es^*} + E_{ind^{**}}$), and (iv) $E_{tot}$ and $E_{disp,exch}$ ($= E_{disp^{**}} + E_{exch^*}$). Insets in (i), (ii), and (iii) are the expanded figures in the region of small values of $-E_{tot}$. Insets in (iv) are the linear regression curves for $E_{tot}$ vs $E_{disp^{**}}$ and $E_{tot}$ vs $E_{exch^*}$. The regression equations with very high degree of correlation are as follows: $E_{tot} = -1.216 + 0.584 \times E_{es^*} - 0.052 \times E_{es^*}^2$ ($R^2$: 0.9798); $E_{tot} = -4.441 + 1.110 \times E_{ind^{**}}$ ($R^2$: 0.9921); $E_{tot} = 0.102 + 0.793 \times E_{es,ind}$ ($R^2$: 0.9967). Thus, if any component of $E_{tot}$, $E_{es}$, $E_{ind^{**}}$, or $E_{es,ind}$ is known, other components can be approximately estimated.

positively charged species have smaller $f_{exch}$, while the displaced stacking complexes such as $\pi$-$\pi$(D), $\pi^+$-$\pi$(D), and $\pi^{+2}$-$\pi$(D) have larger $f_{exch}$ than the corresponding T-shaped complexes.

In the $\pi^+$-$\pi$(D) complexes, the dispersion energy is still a major energy component ($\sim$44%) and the contribution from the electrostatic energy is comparable ($\sim$40%), while the induction energy is still small ($\sim$16%). Meanwhile,

in the $\pi^+$-$\pi$(T) complexes, the dispersion energy is reduced to $\sim$30%, but the induction increases ($\sim$28%), while the electrostatic energy is the major component ($\sim$43%). These complexes are quite similar to the H$^+$-$\pi$(T) complexes, where the dispersion energy is $\sim$26%, the induction energy is $\sim$34%, and the electrostatic energy is $\sim$41%. The $\pi^{++}$-$\pi$(D) complexes have $\sim$29% contribution from the dispersion energy which is smaller than the
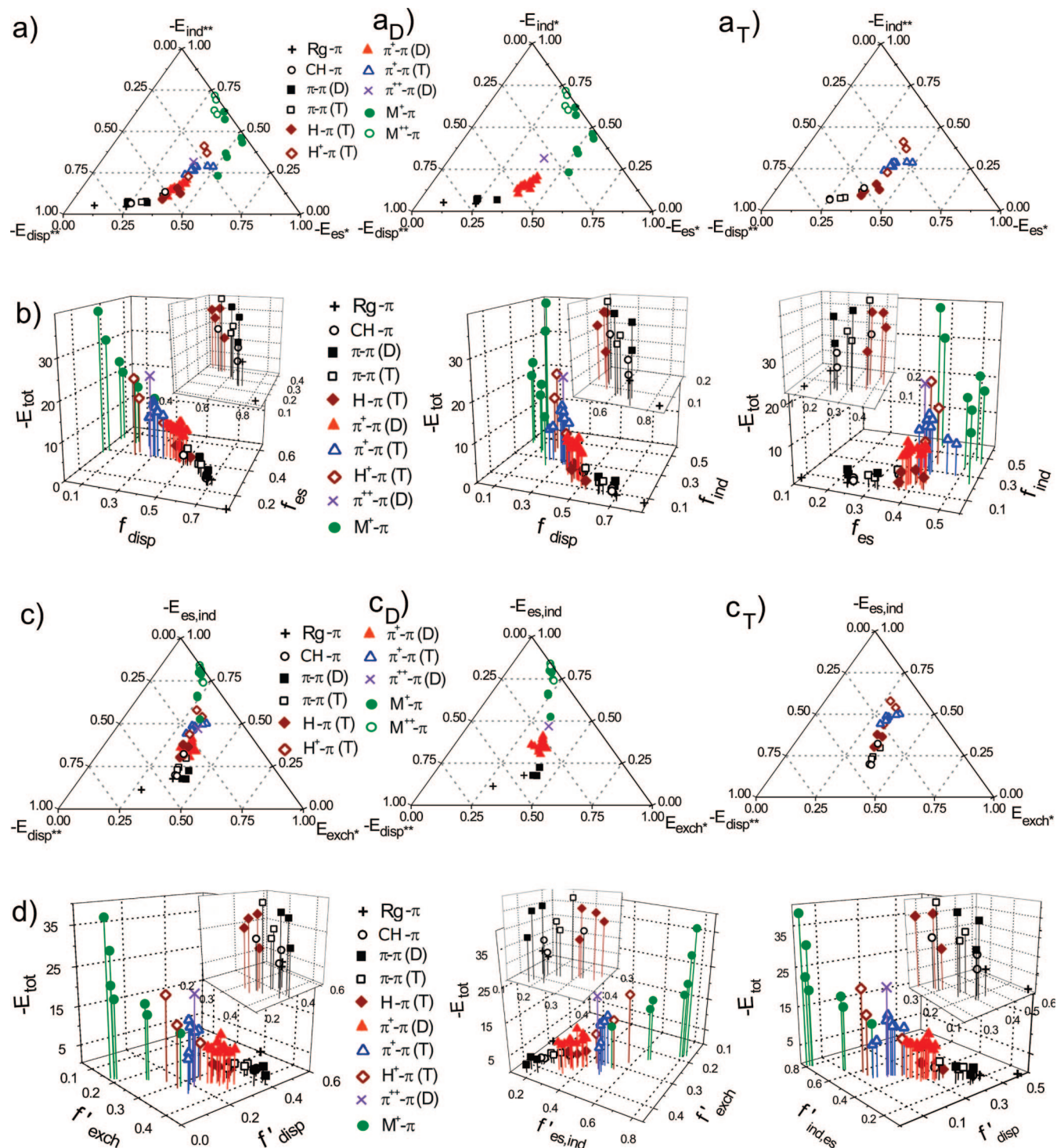
**Figure 5.** (a) Ternary diagrams of the attractive energy component terms ($E_{es^*}$, $E_{ind^{**}}$ and $E_{disp^{**}}$) for the Rg-π, CH-π(T), π-π(D), π-π(T), H-π(T), $π^+$-π(D), $π^+$-π(T), $H^+$-π(T), $π^{+2}$-π(D), $M^+$-π, and $M^{+2}$-π interactions for all the systems studied here (a), for only the displaced stacked systems ($a_D$), and for only the T-shaped systems ($a_T$). (b) 3D-plot of $E_{tot}$ vs any two fractional values $f_{disp}$, $f_{es}$ and $f_{ind}$ of $E_{es^*}$, $E_{ind^{**}}$, and $E_{disp^{**}}$, respectively. (c) Ternary Diagrams plotted using $f_{exch}$, $f_{es,ind}$, and $f_{disp}$ for all the systems studied here (c), for only the displaced stacked systems ($c_D$), and for only the T-shaped systems ($c_T$). (d) 3D-plot of $E_{tot}$ vs any two of $f_{disp}$, $f_{es,ind}$, and $f_{exch}$ [inset for Rg-π, CH-π, H-π(T), and π-π(T)].

contributions from the induction energy (~32%) and the electrostatic energy (~39%).

On the other extreme, the $M^+$-π complexes have small contribution from dispersion energy (~9% except for $Cs^+$ of 23%), large induction energy (~41% except for the moderate value of 23% for $Cs^+$), and very large electrostatic energy (~50%), and the $M^{++}$-π complexes have

very small dispersion energy (~3%), very large induction energy (~66%), and large electrostatic energy (~31%).

When we consider individual π-complexes on the ternary diagram (Figure 5a), there are a few overlapping points between various forms of π-complexes. However, when the displaced-stacked π-complexes along with the stacked metal cation-π complexes (Figure 5$a_D$) are

separated from the T-shaped $\pi$-complexes (Figure 5a$_T$), the $\pi$-$\pi$(D), $\pi^+$-$\pi$(D), $\pi^{+2}$-$\pi$(D), M$^+$-$\pi$, and M$^{+2}$-$\pi$ complexes are well separated from each other except for very few cases.

The 3D-plots of $E_{tot}$ (Figure 5b) with respect to fractional contribution of any two attractive energy components of the ternary diagram (Figure 5a) resolves the overlapping points between $\pi$-$\pi$(T) and $\pi^+$-$\pi$(D) complexes by the differences in height of $E_{tot}$. The $\pi^+$-$\pi$(T) complexes have much smaller heights in $-E_{tot}$ than the $\pi^{+2}$-$\pi$(D) complexes. Though the $\pi^+$-$\pi$(D) and H-$\pi$(T) complexes are partially overlapped on the ternary diagram in Figure 5a, the $\pi^+$-$\pi$(D) complexes have much higher height in $-E_{tot}$ than the H-$\pi$(T) complexes in Figure 5b. One of the closely located points of the Rg-$\pi$ complexes (Kr complex) at the close vicinity of the $\pi$-$\pi$(D) complexes (C$_6$H$_6$ and Tol complexes) is distinguished from the differences in their height of $-E_{tot}$.

Finally, we have drawn a second set of ternary (Figure 5c) diagrams with the inclusion of the exchange repulsion energy terms in addition to the attractive energy components, where the fractional terms are given by $f'_{es,ind} = (E_{es*} + E_{ind**})/(E_{attr} - E_{exch*})$, $f'_{disp} = E_{disp**}/(E_{attr} - E_{exch*})$, and $f'_{exch} = -E_{exch*}/(E_{attr} - E_{exch*})$. Although the M$^{+2}$-$\pi$ complexes have much larger binding energy than the M$^+$-$\pi$ complexes, the ternary diagrams in Figure 5c show that both complexes (with the exception of the Cs$^+$−benzene complex) are clustered on the top of diagrams with the maximum contribution of $-E_{es,ind}$ and the least contributions from $-E_{disp**}$ and $-E_{exch*}$. The Cs$^+$−benzene complex is located close to the $\pi^+$-$\pi$(T), H$^+$-$\pi$(T), and $\pi^{+2}$-$\pi$(D) complex. The $\pi^+$-$\pi$(T), H$^+$-$\pi$, and $\pi^{+2}$-$\pi$(D) complexes are located in the middle of the ternary diagram along the $-E_{es,ind}$ axis. In this context, the $\pi^+$-$\pi$(T) complexes have similar characteristics to non-$\pi$ organic cation-$\pi$ complexes, but are distinctly different from the metallic cation-$\pi$ complexes. This also suggests the importance of the exchange repulsion terms toward the understanding of various $\pi$-systems. The $\pi^+$-$\pi$(D) complexes are located in between the $\pi^+$-$\pi$(T) complexes on the top of the diagram and the $\pi$-$\pi$ complexes on the bottom (Figure 5c). However, the $\pi^+$-$\pi$(D) complexes overlap with the H-$\pi$(T) complexes, and the $\pi^{+2}$-$\pi$(D) complexes overlap with the $\pi^+$-$\pi$(T) and H$^+$-$\pi$(T) complexes. In the ternary diagram of displaced-stacked $\pi$-complexes along with the stacked metal cation-$\pi$ complexes (Figure 5c$_D$), the Rg-$\pi$, $\pi$-$\pi$(D), $\pi^+$-$\pi$(D), $\pi^{+2}$-$\pi$, and (M$^+$-$\pi$, M$^{+2}$-$\pi$) complexes are separated from each other with the exception of the Cs$^+$−benzene complex which lies very close to the $\pi^{+2}$-$\pi$ complex. The overlaps between M$^{+2}$-$\pi$ and the M$^+$-$\pi$ complexes, between Cs$^+$-benzene and the $\pi^{+2}$-$\pi$ complex, and between Kr and C$_6$H$_6$/Tol complexes are distinguished by the differences in height of $-E_{tot}$ (Figure 5d). The C$_2$H$_2$ and NH$_3$ complexes are still located very close to each other with nearly similar heights. Hence, the NH-$\pi$ complex of NH$_3$ is very similar in nature to the CH-$\pi$ complex of C$_2$H$_2$.

On the basis of the above analysis, though the $\pi^+$-$\pi$(T) complexes could be treated in the same category of non-$\pi$ organic cation-$\pi$ complexes, it is however distinctly different from the metallic cation-$\pi$ systems. The $\pi^+$-$\pi$(D) complexes

have different characteristics from the $\pi^+$-$\pi$(T) complexes and are well separated from both the neutral $\pi$-$\pi$(D) complexes with small $E_{ind**}$ or $E_{es,ind}$ on the bottom and the metallic cation M$^+$-$\pi$ complexes with large $E_{ind**}$ or $E_{es,ind}$ on the top in the ternary diagrams (Figure 5, parts a and c). Hence, the $\pi^+$-$\pi$(D) complexes need to be considered as a special type of $\pi$-interaction which lies in between the well-known $\pi$-$\pi$ and cation-$\pi$ complexes.

## 4. Concluding Remarks

On the basis of extensive structural and energetic analysis of various model systems as the representatives of Rg-$\pi$, CH-$\pi$(T), $\pi$-$\pi$(D), $\pi$-$\pi$(T), H-$\pi$(T), $\pi^+$-$\pi$(D), $\pi^+$-$\pi$(T), H$^+$-$\pi$(T), $\pi^{+2}$-$\pi$(D), M$^+$-$\pi$, and M$^{+2}$-$\pi$ interactions, the nature of these interactions is systematically investigated and compared for the similarities and differences between different types of $\pi$-interactions in terms of the energy components. Among all of the energy components, induction energies were found to have the highest correlation with the total binding energies of the $\pi$-complexes, which is followed by electrostatic energies. Although dispersion and repulsive exchange energies independently show very poor correlations with total binding energies, their sum shows an improved correlation with total binding energies due to the cancelation effect. The magnitude of the energy components are important for quantitative understanding of the strength of binding patterns in $\pi$-complexes, while the ternary diagrams employed with selected energy components which show distinctive features for different types of $\pi$-interactions help in clustering different $\pi$-interactions on different spots in the diagrams. The ternary diagrams along with the 3D-plots of $E_{tot}$ with respect to fractional contribution of any two contributing component terms help resolve most of the overlapping points in ternary diagrams for a qualitative and quantitative classification of different $\pi$-complexes except for a few closely overlapped points between CH-$\pi$ and H-$\pi$ complexes which are somewhat similar in characteristics to each other.

From the present comprehensive analysis of various types of $\pi$-interaction, we have demonstrated that the $\pi^+$-$\pi$ interaction is a special type of $\pi$-interaction because the $\pi^+$-$\pi$ complexes show different features from the conventional $\pi$-$\pi$ complexes and cation-$\pi$ complexes (for both organic non-$\pi$ cations and metallic cations). Even the $\pi^+$-$\pi$(D) complexes show different characteristics from the $\pi^+$-$\pi$(T) complexes. The $\pi^+$-$\pi$(D) complexes, which are more commonly observed in the crystal structures than the $\pi^+$-$\pi$(T) complexes, have large dispersion and electrostatic energies and moderate induction energy, while the $\pi^+$-$\pi$(T) complexes have large electrostatic energy and substantial dispersion and induction energies. Namely, the $\pi^+$-$\pi$(D) complexes have larger dispersion energy but smaller induction energy than the $\pi^+$-$\pi$(T) complexes. The $\pi^+$-$\pi$ interaction has both characteristics of conventional $\pi$-$\pi$ and cation-$\pi$ interactions but cannot be represented by their combined interactions. It is much weaker than the commonly known cation-$\pi$ interaction, but much stronger than the $\pi$-$\pi$ interaction.

For the $\pi^+$-$\pi$ complexes with the positively charged $\pi$-system having the (N−H)$^+$ or (C−H)$^+$ group such as in

Comprehensive Energy Analysis for $\pi$-Interaction

*J. Chem. Theory Comput., Vol. 5, No. 3, 2009* **527**

methyl imidazolium, *N*-methyl-guanidinium, pyridinium, and dimethyl imidazolium, the T-shaped structure [$\pi^+$-$\pi$(T) complexes] are more stable than the displaced-stacked structure [$\pi^+$-$\pi$(D) complexes] in the absence of solvent molecules and counteranions, whereas the former tends to be less stable than (or isoenergetic to) the latter in the presence of the solvent molecules and counteranions. This explains why the stacked structures are much more common in the $\pi^+$-$\pi$ interaction. This $\pi^+$-$\pi$ interaction helps in assembling $\pi$-systems since the direct interactions with water or polar solvent molecules are suppressed. We believe that this comprehensive analysis of various types of $\pi$-interaction will be useful for future research works involving $\pi$-interactions in molecular assembly, molecular recognition and sensing, and optimal design of drugs and functional materials.

## Synopsis

A comprehensive energy analysis of various $\pi$-interactions and comparison of their properties in terms of the attractive and repulsive energy components with the aid of ternary diagrams demonstrate that the $\pi_{\text{cation}}$-$\pi$ interaction is a special type of $\pi$-interaction which can be represented by neither the conventional $\pi$-$\pi$ interaction nor the conventional cation-$\pi$ interaction.

**Supporting Information Available:** The calculated isomers on various $\pi_{\text{cation}}$-$\pi$ model systems, details of energetic analysis, and "Complete refs 66 121, and 122. This material is available free of charge via the Internet at http://pubs.acs.org.

### References

(1) Hobza, P.; Selzle, H. L.; Schlag, E. W. *Chem. Rev.* **1994**, *94*, 1767–1784.

(2) Tarakeshwar, P.; Choi, H. S.; Kim, K. S. *Chem. Rev.* **2000**, *100*, 4145–4185.

(3) Brutschy, B. *Chem. Rev.* **2000**, *100*, 3891–3920.

(4) Heβelmann, A.; Jansen, G.; Schütz, M. *J. Am. Chem. Soc.* **2006**, *128*, 11730.

(5) Fiethen, A.; Jansen, G.; Heβelmann, A.; Schütz, M. *J. Am. Chem. Soc.* **2008**, *130*, 1802.

(6) Burley, S. K.; Petsko, G. A. *Science* **1985**, *229*, 23–28.

(7) Gazit, E. *FASEB J.* **2002**, *16*, 77–83.

(8) Hong, B. H.; Lee, J. Y.; Lee, C.-W.; Kim, J. C.; Bae, S. C.; Kim, K. S. *J. Am. Chem. Soc.* **2001**, *123*, 10748–10749.

(9) Meyer, E. A.; Castellano, R. K.; Diederich, F. *Angew. Chem., Int. Ed.* **2003**, *42*, 1210–1250.

(10) Singh, N. J.; Lee, H. M.; Hwang, I.-C.; Kim, K. S. *Supramol. Chem.* **2007**, *19*, 321–332.

(11) Singh, N. J.; Lee, H. M.; Suh, S. B.; Kim, K. S. *Pure Appl. Chem.* **2007**, *79*, 1057–1075.

(12) Hobza, P.; Bludský, O.; Selzle, H. L.; Schlag, E. W. *J. Chem. Phys.* **1992**, *97*, 335–340.

(13) Tarakeshwar, P.; Kim, K. S.; Kraka, E.; Cremer, D. *J. Chem. Phys.* **2001**, *115*, 6018–6029.

(14) Hobza, P.; Selzle, H. L.; Schlag, E. W. *J. Chem. Phys.* **1990**, *93*, 5893–5897.

(15) Kim, K. S.; Tarakeshwar, P.; Lee, J. Y. *J. Am. Chem. Soc.* **2001**, *123*, 3323–3331.

(16) Lee, E. C.; Hong, B. H.; Lee, J. Y.; Kim, J. C.; Kim, D.; Kim, Y.; Tarakeshwar, P.; Kim, K. S. *J. Am. Chem. Soc.* **2005**, *127*, 4530–4537.

(17) Vaupel, S.; Brutschy, B.; Tarakeshwar, P.; Kim, K. S. *J. Am. Chem. Soc.* **2006**, *128*, 5416–5426.

(18) Janowski, T.; Pulay, P. *Chem. Phys. Lett.* **2007**, *447*, 27–32.

(19) Shibasaki, K.; Fujii, A.; Mikami, N.; Tsuzuki, S. *J. Phys. Chem. A* **2007**, *111*, 753–758.

(20) Ringer, A. L.; Figgs, M. S.; Sinnokrot, M. O.; Sherrill, C. D. *J. Phys. Chem. A* **2006**, *110*, 10822–10828.

(21) Tsuzuki, S.; Honda, K.; Fujii, A.; Uchimaru, T.; Mikami, M. *Phys. Chem. Chem. Phys.* **2008**, *10*, 2860–2865.

(22) Tsuzuki, S.; Honda, K.; Uchimaru, T.; Mikami, M.; Tanabe, K. *J. Am. Chem. Soc.* **2000**, *122*, 11450–11458.

(23) Hunter, C. A.; Sanders, J. K. M. *J. Am. Chem. Soc.* **1990**, *112*, 5525–5534.

(24) Hunter, C. A. *Angew. Chem., Int. Ed.* **1993**, *32*, 1584–1586.

(25) Hunter, C. A. *Chem. Soc. Rev.* **1994**, *23*, 101–109.

(26) Cockroft, S. L.; Hunter, C. A.; Lawson, K. R.; Perkins, J.; Urch, C. J. *J. Am. Chem. Soc.* **2005**, *127*, 8594–8595.

(27) Hobza, P.; Selzle, H. L.; Schlag, E. W. *J. Chem. Phys.* **1990**, *93*, 5893–5897.

(28) Hobza, P.; Selzle, H. L.; Schlag, E. W. *J. Phys. Chem.* **1993**, *97*, 3937–3938.

(29) Hobza, P.; Selzle, H. L.; Schlag, E. W. *J. Am. Chem. Soc.* **1994**, *116*, 3500–3506.

(30) Hobza, P.; Selzle, H. L.; Schlag, E. W. *J. Phys. Chem.* **1996**, *100*, 18790–18794.

(31) Špirko, V.; Engkvist, O.; Soldán, P.; Selzle, H. L.; Schlag, E. W.; Hobza, P. *J. Chem. Phys.* **1999**, *111*, 572–582.

(32) Hobza, P.; Sponer, J. *J. Am. Chem. Soc.* **2002**, *124*, 11802–11808.

(33) Sponer, J.; Jurecka, P.; Hobza, P. *J. Am. Chem. Soc.* **2004**, *126*, 10142–10151.

(34) Tsuzuki, S.; Uchimaru, T.; Sugawara, K.-I.; Mikami, M. *J. Chem. Phys.* **2002**, *117*, 11216–11221.

(35) Tsuzuki, S.; Honda, K.; Uchimaru, T.; Mikami, M.; Tanabe, K. *J. Am. Chem. Soc.* **2002**, *124*, 104–112.

(36) Tsuzuki, S.; Uchimaru, T.; Mikami, M. *J. Phys. Chem. A* **2006**, *110*, 2027–2033.

(37) Sinnokrot, M. O.; Valeev, E. F.; Sherrill, C. D. *J. Am. Chem. Soc.* **2002**, *124*, 10887–10893.

(38) Sinnokrot, M. O.; Sherrill, C. D. *J. Phys. Chem. A* **2003**, *107*, 8377–8379.

(39) Sinnokrot, M. O.; Sherrill, C. D. *J. Phys. Chem. A* **2004**, *108*, 10200–10207.

(40) Sinnokrot, M. O.; Sherrill, C. D. *J. Am. Chem. Soc.* **2004**, *126*, 7690–7697.

(41) Sinnokrot, M. O.; Sherrill, C. D. *J Phys Chem A* **2006**, *110*, 10656–10668.

(42) Ringer, A. L.; Sinnokrot, M. O.; Lively, R. P.; Sherrill, C. D. *Chem. Eur. J.* **2006**, *12*, 3821–3828.

(43) Lee, E. C.; Kim, D.; Jurecka, P.; Tarakeshwar, P.; Hobza, P.; Kim, K. S. *J. Phys. Chem. A* **2007**, *111*, 3446–3457.

(44) Dougherty, D. A.; Stauffer, D. *Science* **1990**, *250*, 1558–1560.

(45) Kumpf, R. A.; Dougherty, D. A. *Science* **1993**, *261*, 1708–1710.

(46) Dougherty, D. A. *Science* **1996**, *271*, 163–168.

(47) Ma, J. C.; Dougherty, D. A. *Chem. Rev.* **1997**, *97*, 1303–1324.

(48) Zacharias, N.; Dougherty, D. A. *Trends. Pharmacol. Soc.* **2002**, *23*, 281–287.

(49) Kim, D.; Hu, S.; Tarakeshwar, P.; Kim, K. S.; Lisy, J. M. *J. Phys. Chem. A* **2003**, *107*, 1228–1238.

(50) Lee, J. Y.; Lee, S. J.; Choi, H. S.; Cho, S. J.; Kim, K. S.; Ha, T. K. *Chem. Phys. Lett.* **1995**, *232*, 67–71.

(51) Kim, K. S.; Lee, J. Y.; Lee, S. J.; Ha, T.-K.; Kim, D. H. *J. Am. Chem. Soc.* **1994**, *116*, 7399–7400.

(52) Tsuzuki, S.; Yoshida, M.; Uchimaru, T.; Mikami, M. *J. Phys. Chem. A* **2001**, *105*, 769–773.

(53) Quinonero, D.; Garau, C.; Frontera, A.; Ballester, P.; Costa, A.; Deya, P. M. *J. Phys. Chem. A.* **2005**, *109*, 4632–4637.

(54) Quinonero, D.; Garau, C.; Rotger, C.; Frontera, A.; Ballester, P.; Costa, A.; Deya, P. M. *Angew. Chem., Int. Ed.* **2002**, *41*, 3389–3392.

(55) Kim, D.; Tarakeshwar, P.; Kim, K. S. *J. Phys. Chem. A* **2004**, *108*, 1250–1258.

(56) Kim, D.; Lee, E. C.; Kim, K. S.; Tarakeshwar, P. *J. Phys. Chem. A* **2007**, *111*, 7980–7986.

(57) Kim, D. Y.; Singh, N. J.; Kim, K. S. *J. Chem. Theor. Comput.* **2008**, *4*, 1401–1407.

(58) Janda, K. C.; Hemminger, J. C.; Winn, J. S.; Novick, S. E.; Harris, S. J.; Klemperer, W. *J. Chem. Phys.* **1975**, *63*, 1419–1421.

(59) Vernon, M. F.; Lisy, J. M.; Kwok, H. S.; Krajnovich, D. J.; Tramer, A.; Shen, Y. R.; Lee, Y. T. *J. Phys. Chem.* **1981**, *85*, 3327–3333.

(60) Ruhl, E.; Bisling, P. G. F.; Brutschy, B.; Baumgartel, H. *Chem. Phys. Lett.* **1986**, *126*, 232–237.

(61) Felker, P. M.; Maxton, P. M.; Schaeffer, M. W. *Chem. Rev.* **1994**, *94*, 1787–2160.

(62) Cozzi, F.; Ponzini, F.; Annunziata, R.; Cinquini, M.; Siegel, J. S. *Angew. Chem., Int. Ed.* **1995**, *34*, 1019–1020.

(63) Ren, R.; Jin, Y.; Kim, K. S.; Kim, D. H. *J. Biomol. Struct. Dyn.* **1997**, *15*, 401–405.

(64) Kim, E.; Paliwal, S.; Wilcox, C. S. *J. Am. Chem. Soc.* **1998**, *120*, 11192–11193.

(65) Hong, B. H.; Lee, J. Y.; Cho, S. J.; Yun, S.; Kim, K. S. *J. Org. Chem.* **1999**, *64*, 5661–5665.

(66) Kim, K. S.; et al. *J. Am. Chem. Soc.* **2002**, *124*, 14268.

(67) Nakamura, K.; Houk, K. N. *Org. Lett.* **1999**, *1*, 2049–2051.

(68) Jorgensen, W. L.; Severance, D. L. *J. Am. Chem. Soc.* **1990**, *112*, 4768–4774.

(69) Tarakeshwar, P.; Lee, S. J.; Lee, J. Y.; Kim, K. S. *J. Chem. Phys.* **1998**, *108*, 7217–7223.

(70) Wang, Y.; Hu, X. *J. Am. Chem. Soc.* **2002**, *124*, 8445–8451.

(71) Manojkumar, T. K.; Choi, H. S.; Hong, B. H.; Tarakeshwar, P.; Kim, K. S. *J. Chem. Phys.* **2004**, *121*, 841–846.

(72) Grimme, S. *Chem. Eur. J.* **2004**, *10*, 3423–3429.

(73) Grimme, S. *J. Comput. Chem.* **2004**, *25*, 1463–1473.

(74) Grimme, S. *Angew. Chem., Int. Ed.* **2008**, *47*, 3430–3434.

(75) Manojkumar, T. K.; Kim, D.; Kim, K. S. *J. Chem. Phys.* **2005**, *122*, 014305.

(76) Adamovic, I.; Li, H.; Lamm, M. H.; Gordon, M. S. *J. Phys. Chem. A* **2006**, *110*, 519–525.

(77) Piacenza, M.; Grimme, S. *J. Am. Chem. Soc.* **2005**, *127*, 14841–14848.

(78) Mishra, B. K.; Sathyamurthy, N. *J. Phys. Chem. A* **2005**, *109*, 6–8.

(79) Diastro, R. A.; von Helden, G.; Steele, R. P.; Head-Gordon, M. *Chem. Phys. Lett.* **2007**, *437*, 277–283.

(80) Zhao, Y.; Truhlar, D. G. *J. Phys. Chem. A* **2005**, *109*, 4209–4212.

(81) Heβelmann, A.; Jansen, G.; Schütz, M. *J. Chem. Phys.* **2005**, *122*, 014103.

(82) Piacenza, M.; Grimme, S. *Chem. Phys. Chem.* **2005**, *6*, 1554–1558.

(83) Podeszwa, R.; Bukowski, R.; Szalewicz, K. *J. Phys. Chem. A* **2006**, *110*, 10345–10354.

(84) Sato, T.; Tsuneda, T.; Hirao, K. *J. Chem. Phys.* **2005**, *123*, 104307.

(85) Zhao, Y.; Truhlar, D. G. *Acc. Chem. Res.* 2008, DOI: 10.1021/ar700111a.

(86) Levy, C. W.; Roujeinikova, A.; Sedelnikova, S.; Baker, P. J.; Stuitje, A. R.; Slabas, A. R.; Rice, D. W.; Rafferty, J. B. *Nature* **1999**, *398*, 383–384.

(87) Marcotrigiano, J.; Gingras, A. C.; Sonenberg, N.; Burley, S. K. *Cell* **1997**, *89*, 951–961.

(88) Schumacher, M. A.; Miller, M. C.; Grkovic, S.; Brown, M. H.; Skurray, R. A.; Brennan, R. G. *Science* **2001**, *294*, 2158–2163.

(89) Biot, C.; Buisine, E.; Rooman, M. *J. Am. Chem. Soc.* **2003**, *125*, 13988–13994.

(90) Kapoor, L. S M.; Surolia, N.; Surolia, A.; Suguna, K. *J. Mol. Biol.* **2004**, *343*, 147–155.

(91) Murray, D. S.; Schumacher, M. A.; Brennan, R. G. *J. Biol. Chem.* **2004**, *279*, 14365–14371.

(92) Ghosh, P.; Park, C.; Peterson, M. S.; Bitterman, P. B.; Polunovsky, V. A.; Wagner, C. R. *Bioorg. Med. Chem. Lett.* **2005**, *15*, 2177–2180.

(93) Crowley, P. B.; Golovin, A. *Proteins* **2005**, *59*, 231–239.

(94) Argiriadi, M. A.; Morisseau, C.; Hammock, B. D.; Christianson, D. W. *Proc. Natl. Acad. Sci. U.S.A.* **1999**, *96*, 10637–10642.

(95) Thomas, A.; Meurisse, R.; Charloteaux, B.; Brasseur, R. *Proteins* **2002**, *48*, 628–634.

(96) Li, H. L.; Galue, A.; Meadows, L.; Ragsdale, D. S. *Mol. Pharmacol.* **1999**, *55*, 134–141.

Comprehensive Energy Analysis for $\pi$-Interaction

*J. Chem. Theory Comput., Vol. 5, No. 3, 2009* **529**

(97) Okada, A.; Miura, T.; Takeuchi, H. *Biochemistry* **2001**, *40*, 6053–6060.

(98) Wintjens, R.; Lievin, J.; Rooman, M.; Buisine, E. *J. Mol. Biol.* **2000**, *302*, 395–410.

(99) Biot, C.; Wintjens, R.; Rooman, M. *J. Am. Chem. Soc.* **2004**, *126*, 6220–6221.

(100) Stoddart, J. F. *Pure Appl. Chem.* **1998**, *60*, 467–472.

(101) Odell, B.; Reddington, M. V.; Slawin, A. M. Z.; Spencer, N.; Stoddart, J. F.; Williams, D. J. *Angew. Chem., Int. Ed.* **1998**, *27*, 1547–1550.

(102) Raymo, F. M.; Stoddart, J. F. *Chem. Rev.* **1999**, *99*, 1643–1663.

(103) Rowan, S. J.; Cantrill, S. J.; Cousins, G. R. L.; Sanders, J. K. M.; Stoddart, J. F. *Angew. Chem. Int. Ed.* **2002**, *41*, 898–952.

(104) Kaifer, A. E. *Acc. Chem. Res.* **1999**, *32*, 62–71. Balzani, V.; Credi, A.; Raymo, F. M.; Stoddart, J. F. *Angew. Chem., Int. Ed.* **2000**, *39*, 3349–3391.

(105) Nelson, A.; Belitsky, J. M.; Vidal, S.; Joiner, C. S.; Baum, L. G.; Stoddart, J. F. *J. Am. Chem. Soc.* **2004**, *126*, 11914–11922.

(106) Yamada, S.; Morita, C. *J. Am. Chem. Soc.* **2002**, *124*, 8184–8185.

(107) Birman, V. B.; Uffman, E. W.; Jiang, H.; Li, X.; Kilbane, C. J. *J. Am. Chem. Soc.* **2004**, *126*, 12226–12227.

(108) Petti, M. A.; Shepodd, T. J.; Barrans, R. E., Jr.; Dougherty, D. A. *J. Am. Chem. Soc.* **1988**, *110*, 6825–6840.

(109) Dupont, J.; de Souza, R. F.; Suarez, P. A. Z. *Chem. Rev.* **2002**, *102*, 3667–3692.

(110) Hu, Z.; Margulis, C. J. *Proc. Natl. Acad. Sci. U.S.A.* **2006**, *103*, 831–836.

(111) Abouderbala, L. O.; Belcher, W. J.; Boutelle, M. G.; Cragg, P. J.; Steed, J. W.; Turner, D. R.; Wallace, K. J. *Proc. Natl. Acad. Sci. U.S.A.* **2002**, *99*, 5001–5006.

(112) Chellapan, K.; Singh, N. J.; Hwang, I. C.; Lee, J. W.; Kim, K. S. *Angew. Chem., Int. Ed.* **2005**, *44*, 2899–2903. (a) *Angew. Chem.* 2005, *117*, 2959–2963.

(113) Yoon, J.; Kim, S. K.; Singh, N. J.; Kim, K. S. *Chem. Soc. Rev.* **2006**, *35*, 355–360.

(114) Gallivan, J. P.; Dougherty, D. A. *Proc. Natl. Acad. Sci. U.S.A.* **1999**, *96*, 9459–9464.

(115) Cauët, E.; Rooman, M.; Wintjens, R.; Liévin, J.; Biot, C. *J. Chem. Theory. Comput.* **2005**, *1*, 472–483.

(116) Tsuzuki, S.; Mikami, M.; Yamada, S. *J. Am. Chem. Soc.* **2007**, *129*, 8656–8662.

(117) Singh, N. J. Ph. D *dissertation*, Pohang University of Science and Technology, 2005, 123−156.

(118) Kim, K. S. Creative Research Initiative Proposal (KOSEF), 2005.

(119) Helgaker, T.; Klopper, W.; Koch, H.; Noga, J. *J. Chem. Phys.* **1997**, *106*, 9639–9646.

(120) Min, S. K.; Lee, E. C.; Lee, H. M.; Kim, D. Y.; Kim, D.; Kim, K. S. *J. Comput. Chem.* **2008**, *29*, 1208–1221.

(121) *Gaussian 03, Revision C.02*, Frisch, M. J. et al., Gaussian, Inc., Wallingford CT, 2004.

(122) MOLPRO, version 2006.1. a package of *ab initio* programs, Werner, H.-J. et al.

(123) SAPT 2006: "An *Ab Initio* Program for Many-Body Symmetry-Adapted Perturbation Theory Calculations of Intermolecular Interaction Energies", Bukowski R.; Cencek, W.; Jankowski, P.; Jeziorski, B.; Jeziorska, M.; Kucharski, S. A.; Lotrich, V. F.; Misquitta, A. J.; Moszynski, R.; Patkowski, K.; Podeszwa, R.; Rybak, S.; Szalewicz, K.; Williams, H. L.; Wheatley, R. J.; Wormer, P. E. S.; ·Zuchowski, P. S.

(124) Jeziorski, B.; Moszynski, R.; Szalewicz, K. *Chem. Rev.* **1994**, *94*, 1887–1930.

(125) He$\beta$elmann, A.; Jansen, G.; Schütz, M. *J. Chem. Phys.* **2005**, *122*, 014103.

(126) Lee, H. M.; Suh, S. B.; Lee, J. Y.; Tarakeshwar, P.; Kim, K. S. *J. Chem. Phys.* **2000**, *112*, 9759–9772.

(127) Allen, F. H. *Acta Crystallogr. B* **2002**, *58*, 380–388.

(128) Allen, F. H.; Motherwell, W. D. S. *Acta Crystallogr., B* **2002**, *58*, 407–422.

(129) Shen, H. W.; Eisenberg, A. *J. Phy. Chem. B* **1999**, *103*, 9473–9487.

CT800471B